# Methodology for Ensuring Safety and Operational Reliability of Reusable Launch Vehicle Composite Structures under High-Intensity Vibroacoustic Loads

**Maryna Khamlak**

# Methodology for Ensuring Safety and Operational Reliability

## of Reusable Launch Vehicle Composite Structures under High-Intensity Vibroacoustic Loads


**Maryna Khamlak**

**Faculty of Aviation and Rocket-Space Engineering**

**National Aerospace University "Kharkiv Aviation Institute"**

**City, Country: Kharkiv, Ukraine**



## Publication Info

THE AMERICAN JOURNAL OF ENGINEERING AND TECHNOLOGY

(ISSN: 2693-0811)

**ISBN:** 978-1-957653-66-2

**CROSSREF DOI:** https://doi.org/10.37547/tajet/book-26-01

**PUBLISHED DATE:** 09 June 2026

## Preface

The monograph examines a probabilistic, damage-tolerant methodology for ensuring the safety and operational reliability of reusable launch vehicle composite structures subjected to high-intensity vibroacoustic loads. The study is motivated by the rapid expansion of reusable launch systems, for which mass efficiency, certification speed, and interflight survivability of composite payload fairings have become decisive engineering and economic constraints. The aim of the monograph is to develop and substantiate an integrated analytical framework for predicting residual life, defect evolution, and safe operating margins in large-scale orthotropic shell structures under stochastic acoustic excitation. The scientific novelty lies in the synthesis of hybrid FE-SEA vibroacoustic modeling, stochastic fracture mechanics, XFEM/VCCT-based defect-growth simulation, and nondestructive-evaluation data fusion within a single closed assessment cycle. The principal conclusion is that deterministic metallic-style safety approaches are inadequate for heterogeneous composites; instead, probabilistic life prediction enables more credible certification, targeted inspection planning, reduced unnecessary mass, and a justified extension of reusable fairing service life without compromising mission safety. The monograph will be useful for researchers, design engineers, certification specialists, and graduate students in aerospace structures and composite mechanics.

# INTRODUCTION

The contemporary stage of aerospace industry development is defined by a fundamental transition from expendable launch vehicles to reusable launch vehicle (RLV) systems (Du et al., 2025), which is reshaping both engineering practice and economic models. This transition is driven by rapid growth in the global space economy, including the expansion of near-Earth orbital infrastructure, broadband satellite megaconstellations, and commercial deep-space exploration activities. According to recent industry data, the global space economy reached USD 613 billion in 2024, with approximately 78% of this growth originating from the commercial sector (Space Foundation, 2025). As a result, reusable systems are no longer a technological option but a central requirement for competitiveness and scalability in modern space operations.

The economic model of reusable launch vehicles is predicated on two critical imperatives: maximizing payload capacity by minimizing the airframe's dry mass, and minimizing turnaround time and cost between flights (Kang et al., 2025). To attain these indicators, polymer composite materials, PCMs, are being employed ever more extensively in the design of highly loaded assemblies, first and foremost, payload fairings, abbreviated as PF (Upganlawar & Anasane, Sandeep S, 2026). The use of advanced carbon-fiber-reinforced plastics enables substantial improvements in the structural weight efficiency owing to their outstanding specific strength and stiffness (Mamat et al., 2025).

However, the incorporation of composite materials into the architecture of reusable systems poses a fundamental scientific and technological challenge: fatigue degradation and the progressive reduction in the residual strength of PCMs under the influence of extreme operational factors (Alamry, 2024). In contrast to the metallic alloys traditionally used in rocketry, composites exhibit pronounced structural heterogeneity and anisotropy, which fundamentally determine different mechanisms of damage accumulation (Huang & Bobyr, 2023). In practical terms, this manifests as substantially greater statistical scatter in strength. Composites made under laboratory conditions have a strength coefficient of variation of 3 to 20 percent, while aerospace sheet aluminum alloys have a coefficient of variation of 2 to 4 percent. Structurally, composites are statistically less homogeneous than a metal, and the uncertainties of a composite's load-bearing behavior are increased in the presence of manufacturing defects.

This makes deterministic methods, commonly used for metals, unsuitable for use on PCMs, which leads to underestimating the failure probability if no probabilistic correction is applied (Elhajjar, 2025). Payload fairings are subjected to intense vibroacoustic loads during launch and transonic flight, resulting from the jet plume of the main engine and the aerodynamic pulsations (Ahn & Lee, 2022). Under the influence of stochastic acoustic fields, technological microdefects that inevitably arise during the manufacture of large-scale layered structures can undergo unpredictable coalescence and macroscopic, avalanche-like growth. This places the overall safety of the space mission at risk, thereby rendering the problem of predicting PCM behavior under acoustic loading one of the most acute issues in contemporary aerospace mechanics.

Despite the extensive body of research in layered composite mechanics, contemporary engineering practice still lacks sufficiently validated analytical tools for predicting structural behavior under realistic operating conditions. The central problem is the absence of a unified and scientifically substantiated methodology capable of predicting the kinetics of manufacturing-defect growth in composite shell structures subjected to stochastic acoustic loading. Existing approaches remain fragmented, typically addressing isolated aspects of the problem rather than providing an integrated predictive framework.

Existing approaches to the strength assessment of aerospace structures are often based on deterministic quasi-static models or spectral methods developed for isotropic materials. These methods are incapable of adequately describing the complex dynamic response of an orthotropic heterogeneous medium to broadband random acoustic excitation. The application of traditional generalized safety factors borrowed from metallic aircraft engineering gives rise to a fundamental contradiction. It either causes an excessive increase in the mass of the payload fairing structure, thereby nullifying all weight-related advantages of using PCMs, or results in an underestimation of the risks of sudden catastrophic failure due to the uncontrolled growth of hidden interlaminar delaminations (Huang & Bobyr, 2023). The stochastic nature of both the vibroacoustic impact and the initial distribution of technological defects in large-scale parts formed by automated layup methods necessitates an urgent transition to probabilistic methods of fracture mechanics and to the concept of design with allowable damage tolerance.

The **aim** of this study is to develop and rigorously substantiate an integrated methodology for assessing the residual life and survivability of large-scale composite shell structures, with particular focus on payload fairings of reusable launch vehicles fabricated from polymer composite materials and operating under high-intensity vibroacoustic loading. The proposed methodology systematically integrates advanced computational fracture mechanics, probabilistic statistical analysis, and hybrid vibroacoustic modeling into a unified predictive framework, enabling reliable evaluation of defect evolution, structural integrity, and safe operational limits of RLV systems under realistic service conditions.

The **object** of the study comprises highly loaded thin-walled composite shell structures for aerospace applications operating under extreme dynamic conditions, the principal representative of which is the large-scale payload fairing of reusable space transportation systems.

The **subject** of the study is the mechanics and kinetics of the spatial development of macroscopic defects, fatigue cracks, interlaminar delaminations, and matrix microcracks in orthotropic layered media under conditions of a complex stochastic stress-strain state initiated by intense broadband vibroacoustic loading over the powered phases of the launch vehicle trajectory.

From a systems engineering perspective, the proposed methodology establishes a closed and integrated analytical cycle that links design, structural analysis, defect evolution, and certification processes for composite airframe elements in reusable launch vehicles. The practical and systemic significance of this work is multi-dimensional.

First, the methodology enables a significant improvement in operational reliability and mission safety by providing accurate prediction of defect kinetics and the conditions under which defects reach critical size, thereby supporting the development of scientifically justified interflight nondestructive inspection strategies.

Second, the use of validated hybrid numerical models that combine vibroacoustic analysis with fracture mechanics substantially reduces both the time and cost associated with design and verification, while minimizing reliance on expensive full-scale testing in reverberation chambers.

Third, the methodology provides a transparent and physically grounded analytical basis for demonstrating structural survivability, which is essential for accelerating certification processes under regulatory frameworks in aerospace systems. In a highly competitive commercial launch market, reducing certification timelines directly contributes to economic efficiency and program viability.

Finally, the transition from conservative deterministic safety factors to probabilistic, defect-informed design approaches enables targeted mass optimization of composite structures, resulting in increased payload capacity and improved economic performance of reusable launch vehicle missions.

# CHAPTER 1.
# Strength and Reliability Problems of Composite Structures in Contemporary Aerospace Engineering

The developmental context of the contemporary aerospace industry, particularly in the United States and the countries of the European Union, is inseparably bound up with an uncompromising struggle to reduce the dry mass of the airframe and to increase the economic return of spacecraft (Pazhani et al., 2024). However, the experience gained in developing advanced commercial launch vehicles unequivocally demonstrates that traditional approaches to reliability assurance, based on simple quasi-static calculations and enormous safety factors, have exhausted their effectiveness (Wagenblast & Bettinger, 2024). To satisfy reusability requirements, a thorough understanding of the physics of the processes unfolding within the structure under real flight conditions is required. This chapter substantiates the necessity of abandoning design for infinite life in favor of the safe-damage paradigm, and also provides a detailed analysis of the fundamental problems of the behavior of composite materials under the action of specific stochastic loads.

## 1.1. Loading Specificity of Payload Fairings

The problem of minimizing dynamic stresses and strains in thin-walled shells is a central task in aerospace structural dynamics (Ahn & Lee, 2022). The payload fairing, representing a large-scale stiffened composite shell, performs the critical function of protecting an expensive payload from the oncoming aerodynamic flow, kinetic heating, and acoustic exposure. During launch and passage through the atmospheric segment of the trajectory, the fairing functions under conditions of extreme multifactor dynamic excitation, the principal damaging agent of which is sound pressure of colossal intensity.

The vibroacoustic analysis of the fairing structure is strictly mandatory for the two most hazardous flight regimes: the moment of liftoff of the launch vehicle from the launch complex and motion in the transonic-speed zone, coinciding with traversal of the region of maximum aerodynamic pressure.

At launch, the first-stage engines generate a high-intensity supersonic jet plume that produces strong pressure fluctuations and broadband acoustic excitation. The sound waves emitted from the nozzles are reflected by flame trenches and structural elements of the launch platform (Escartí-Guillem et al., 2024), resulting in multiple reflections and amplification of the acoustic field. This process forms a high-energy, diffuse acoustic environment that envelops the entire launch vehicle, including the payload fairing. Under these conditions, sound pressure levels on the shell surface typically exceed 140–150 dB, creating severe dynamic loading that directly influences structural response and fatigue behavior (Escartí-Guillem et al., 2024).

At the same time, the spectral localization of the load is critical for the payload and the fairing's internal cavity. The analysis of the spectral localization of acoustic loading requires consideration of the excitation level and of the structural configuration of the sound-absorbing and sound-insulating means employed. Within the NEMFAT test series, several variants of the acoustic protection architecture were considered, differing in melamine foam layer thickness, the presence of voids, mass inclusions, and an internal barrier layer (Hughes et al., 2014). These configurations provide a basis for subsequent comparison of their transmission losses across different frequency ranges. Figure 1 shows cross-sectional schematics of the NEMFAT configurations tested for sound insulation assessment.

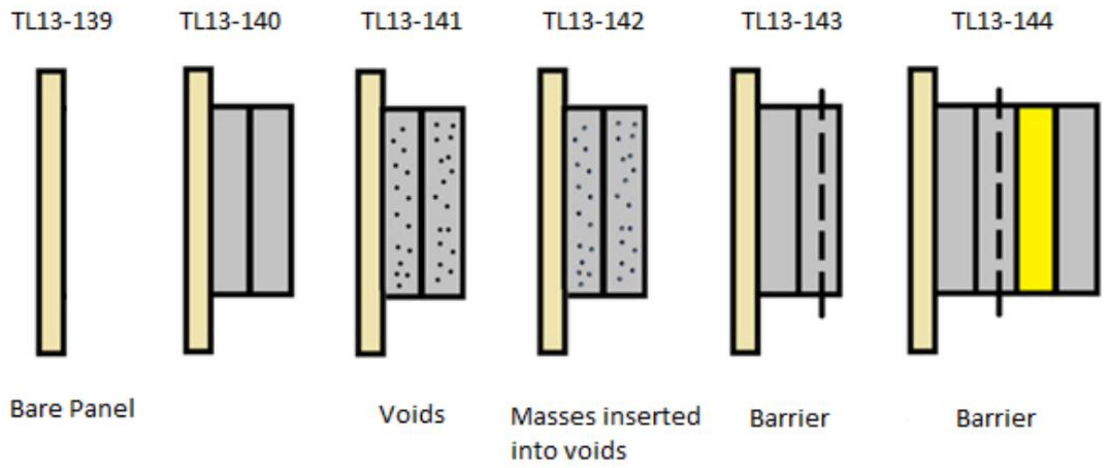


**Fig. 1.** Cross-sectional Views of NEMFAT TL Test Configurations (Hughes et al., 2014)

For prospective NASA heavy-lift systems, it was noted that the internal acoustic levels in the fairing may be up to 10 dB higher than those of typical commercial ELV, while the 20–400 Hz band is considered the most hazardous. It is precisely within this range that the most sensitive resonant interactions are formed among the shell, the internal air, and the installed payload (Hughes et al., 2014).

To assess the effectiveness of different acoustic protection options, it is expedient to consider the frequency dependence of the sound insulation coefficient for several fairing-panel configurations with melamine foam. As the NEMFAT tests demonstrated, the greatest increase in TL occurs predominantly above 200 Hz, whereas in the low-frequency region below 100 Hz, the differences among the investigated configurations are substantially smaller. This confirms that low frequencies remain the most problematic part of the internal acoustic environment of the payload fairing. Figure 2 presents the NEMFAT transmission loss test results for different acoustic treatment options.

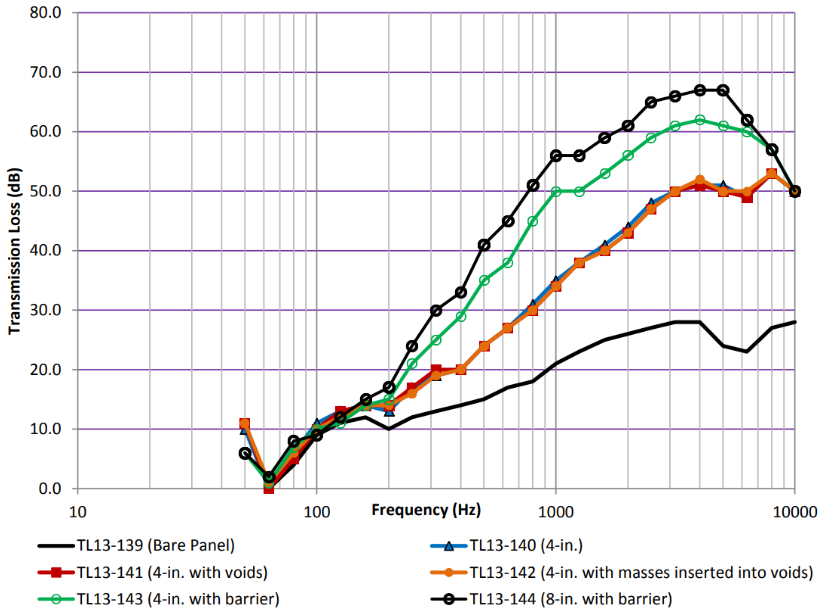


**Fig. 2.** NEMFAT TL Test Results (Hughes et al., 2014)

The second critical loading phase begins when the rocket overcomes the sound barrier. In the transonic regime, unsteady shock waves and regions of intense separated flow form on the surface of the composite fairing. The turbulent boundary layer generates powerful aerodynamic noise, which leads to broadband stochastic vibrations of the thin-walled shell. Acoustic oscillations at both stages exhibit a continuous frequency spectrum approximating white or pink noise over several hertz to tens of kilohertz (Gee et al., 2023).

Since the vibroacoustic excitation of the fairing is broadband, it is fundamentally important to compare them with computational predictions. Such a comparison enables assessing the applicability of numerical models for the preliminary design of acoustic protection and identifying the frequency ranges at which the computation begins to diverge from the experiment. In the NEMFAT tests, it was shown that the predictions of the VA One model are in good agreement with the experimental data up to frequencies on the order of 1000 Hz, whereas at higher frequencies, the calculated curves continue to rise while the experimental data reach a plateau. Figures 3 and 4 compare the RAL experimental data with preliminary VA One computational predictions for two acoustic-treatment configurations.

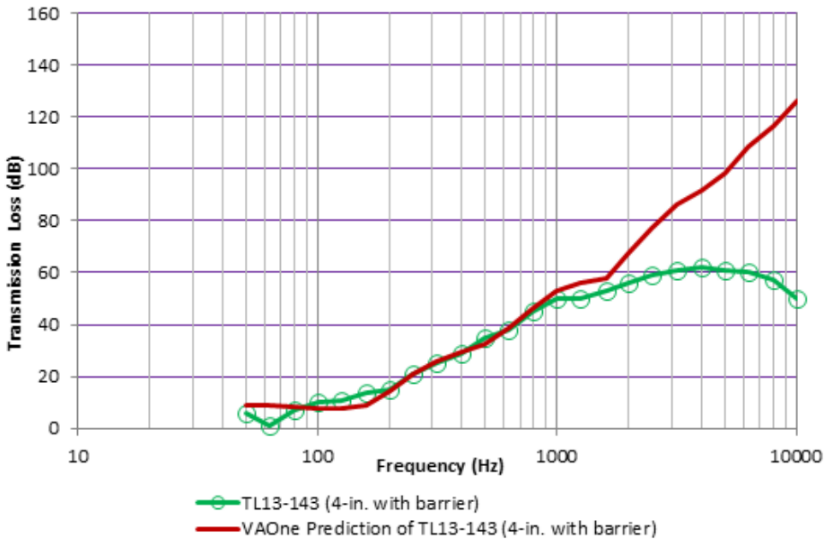


**Fig. 3.** 4-in. ML foam with mass barrier, TL13-143 (Hughes et al., 2014)

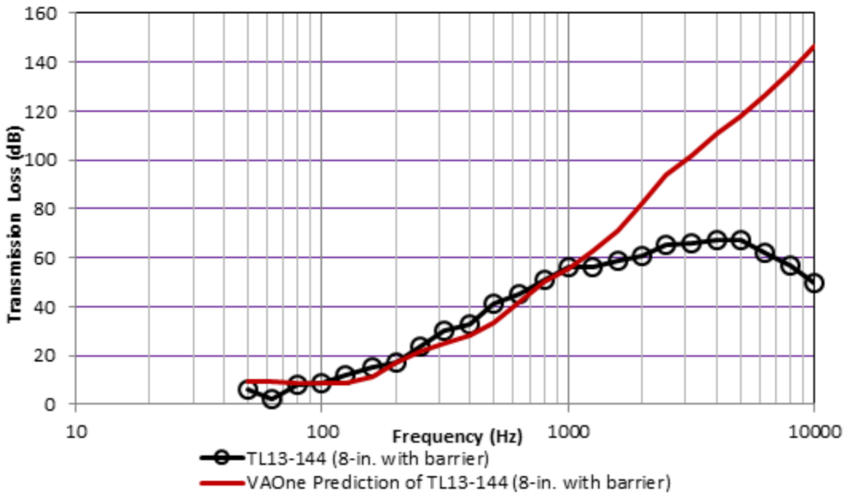


**Fig. 4.** 8-in. combination foam treatment, TL13-144 (Hughes et al., 2014)

A critical engineering consideration is that within the broadband acoustic excitation spectrum, frequency components frequently coincide with the natural frequencies of the fairing’s flexural modes, resulting in resonance phenomena (Ahn & Lee, 2022). In practical terms, this means that structural risk is concentrated within specific frequency bands rather than distributed uniformly across the spectrum. In contemporary analysis of payload fairings, the frequency range of 20–200 Hz is typically treated as low-frequency and analyzed using deterministic finite element methods; the 200–500 Hz band represents a transition region addressed through hybrid FE-SEA approaches; and the 500 Hz–10 kHz range is considered high-frequency, where statistical energy analysis methods dominate. For composite shell structures, the first natural modes often occur at frequencies on the order of tens of hertz; for example, configurations similar to STARS/Minotaur exhibit first shell modes near 75 Hz. As a result, even low-frequency acoustic excitation can efficiently transfer energy into the structure, leading to significant dynamic response and accelerated fatigue damage accumulation.

This inevitably leads to the emergence of both local and global spatial resonances.

Given the high frequency of deformation cycles, fatigue damage accumulation in the polymer matrix and at the fiber–matrix interface proceeds extremely rapidly, thereby determining the distinctly fatigue-related character of composite degradation.

The action of the external acoustic field causes flexural vibrations of the shell, which, in turn, reradiate sound energy into the internal volume of the fairing, thereby forming an internal acoustic field. The modeling of this process is complicated by the so-called acoustic fill effect, the phenomenon of changes in sound pressure levels inside the cavity in the presence of a payload therein as compared with an empty shell.

According to regulatory documentation, particularly NASA-STD-7001B, the analytical calculation of the fill factor depends on the ratio of the satellite volume to the fairing volume and the magnitude of the gap between them (Shearer & Bittinger, 2022).

In practice, this is not a secondary correction. Using the example of a payload in the 8.4-meter SLS Block 1B fairing, NASA separately showed that the presence of the payload alters the internal distribution of sound pressure levels relative to an empty cavity (Shearer & Bittinger, 2022). Therefore, a flight-level prediction without fill correction is considered insufficiently reliable. In other words, even under the same external acoustics, the empty and filled fairings create different internal acoustic regimes.

This difference is especially noticeable when comparing the averaged acoustic pattern across the entire internal cavity with the local acoustic environment near the payload. The simulation results for the 8.4-meter SLS Block 1B fairing show that, given the known shape and dimensions of the payload, it is more correct to characterize the internal acoustic environment by the zone of interest directly adjacent to the payload. Thus, it is confirmed that the presence of the payload changes the spatial distribution of sound pressure inside the fairing. The figure 5 compares the averaged SPL levels in the zone of interest near the payload and across the entire internal cavity of the fairing.

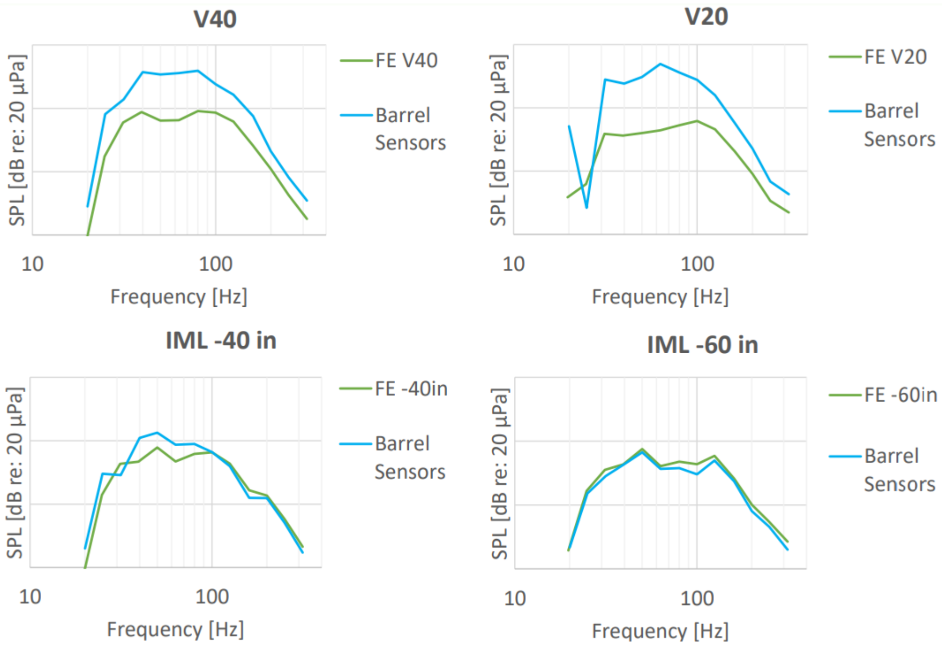


**Fig. 5.** Comparison of zone of interest and overall cavity averages (Shearer & Bittinger, 2022)

However, contemporary studies show that classical calculation methods encounter significant difficulties in the low-frequency range, where the basic assumptions underlying the diffuseness of the acoustic field are violated (Dash et al., 2024). The spatial variability of pressure leads to the formation of axially oriented standing waves, creating nonuniform, difficult-to-predict zones of peak stress within the composite fairing itself.

Historically, the only reliable method for assessing acoustic strength was the conduct of expensive full-scale physical tests in giant reverberation chambers (Shimazaki & Shi, 2021). At the early design stage of commercial RLVs, this approach is economically inefficient. Today, the industry is moving toward complex computational frameworks.

The significance of such tests is clearly visible in examples of real fairing acoustic programs. Thus, in the Cassini/Titan IV tests, one objective was to experimentally confirm a 3 dB reduction in the acoustic environment at 200 and 250 Hz relative to the baseline blanket configuration. For payload fairings, this is of principal importance, since even a reduction of several decibels within a narrow critical band can noticeably reduce dynamic stresses in the most sensitive regions of the shell and the load on the payload.

For the low-frequency range, usually up to 200–400 Hz, where the modal density of the structure is relatively low, deterministic Finite Element Method, FEM, and Boundary Element Method, are used (Dash et al., 2024). FEM enables a detailed description of the stress-strain state of the layered shell. However, as frequency increases, the flexural wavelength decreases, and ensuring FEM convergence requires exponential mesh refinement, which renders the calculations computationally prohibitive.

The dispersive character of flexural-wave propagation is well illustrated by experimental time signals recorded at two points of a rod. As the impulse propagates, its shape becomes noticeably distorted and stretched in time: the high-frequency components, possessing greater velocity, arrive earlier, whereas the low-frequency ones arrive later. Such behavior reflects the frequency dependence of the wave parameters of the flexural wave and, in the context of numerical modeling, indicates the necessity of finer spatial resolution when transitioning to high frequencies, as shown in Figure 6.

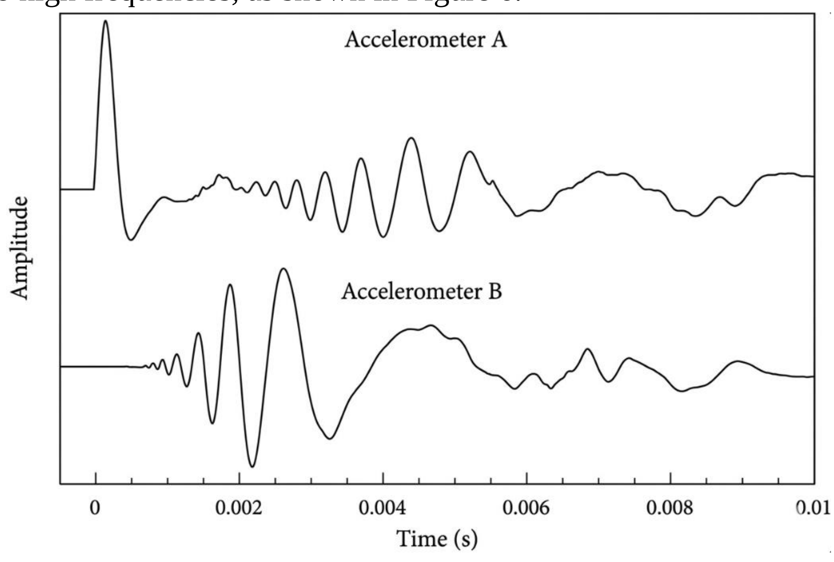


**Fig. 6.** Dispersive propagation of a flexural wave in a rod (Russell, n.d.)

For the high-frequency spectrum, Statistical Energy Analysis, SEA, is applied. SEA operates with flows of averaged vibrational energy between subsystems (Borgaonkar et al., 2021). The advanced global standard in RLV design is the creation of combined FE-SEA hybrid models, in which low-frequency dynamics and rigid load-bearing frames are modeled through FEM, whereas acoustic cavities and high-frequency oscillations of thin composite skins are represented through SEA subsystems (Ahn & Lee, 2022). Figure 7 shows the physical-mechanical model of vibroacoustic loading of the payload fairing and degradation of the composite structure.

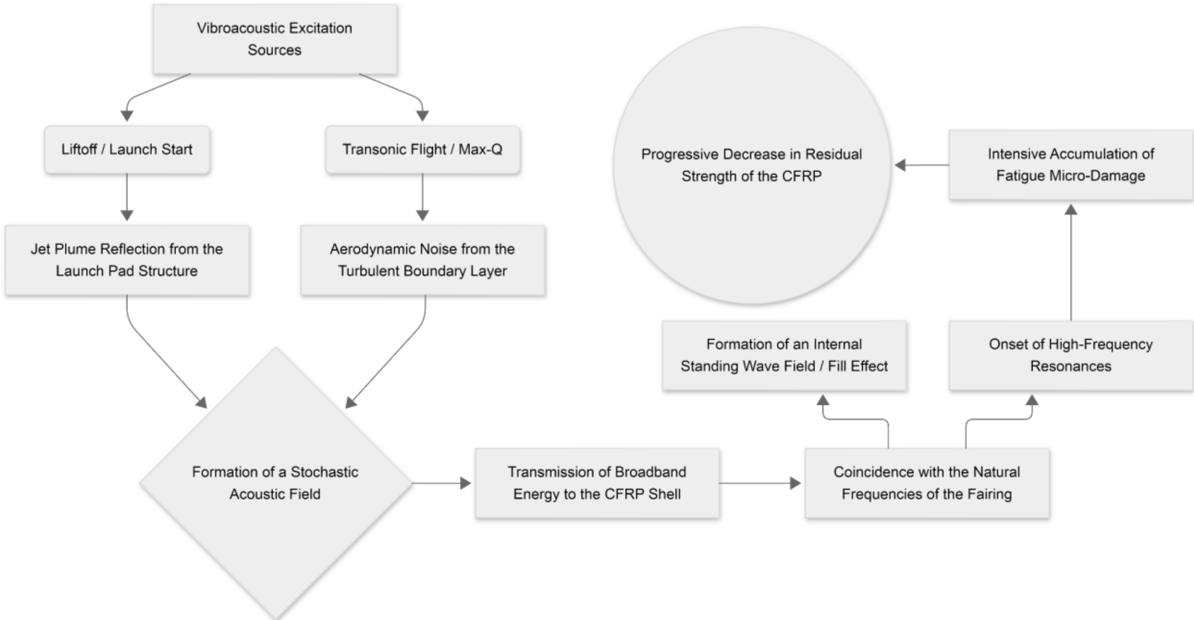


**Fig. 7.** Physical and mechanical model of vibroacoustic loading of the payload fairing and degradation of the composite structure

## 1.2. The Damage Tolerance Concept in Aerospace Engineering

For decades, the classical design of load-bearing structures in aviation and space engineering was based on the safe-fatigue-life paradigm (Hoole et al., 2020). This approach presupposed the creation of a structure capable of withstanding the design load spectrum without macroscopic cracks throughout the prescribed service life. Any detected crack automatically classifies the part as rejected. However, the specificity of modern layered composites, technologically predisposed to microdefect formation, as well as the extremely stringent requirements for minimizing the passive mass of reusable launch vehicles, necessitated a fundamental change in engineering philosophy.

In the United States, and subsequently in other leading aerospace powers, a full-scale transition occurred toward design based on the concept of safe damage tolerance or survivability - Damage Tolerance, DT (Peishi et al., 2021). The Damage Tolerance concept is based on the explicit assumption that structural defects are inherently present from manufacturing or will develop during operation, including forms of hidden damage such as Barely Visible Impact Damage (BVID) (Adams & Engle, 1985). Under this paradigm, the role of the structural engineer is not to eliminate defects, but to design the structure such that defect growth remains stable and does not reach critical size before detection or the end of the intended service life. This approach requires predictive modeling of defect evolution, integration with inspection capabilities, and quantitative assessment of residual strength, ensuring that structural integrity is maintained throughout operation despite the presence of damage.

Although the DT concept was borrowed from commercial aviation, its adaptation for space engineering presents fundamental distinctions. The fundamental difference lies in the life-cycle profile: unlike aircraft, which undergo regular depot inspections and repairs, up to 75,000 cycles over 30 years, spacecraft have no possibility for inspection and structural restoration after liftoff from the launch table (Raju et al., 2010). Consequently, space regulators have adopted much more conservative requirements to ensure residual strength.

In the United States, the basic regulatory document is NASA-STD-5019A (NASA, 2025). This standard establishes that fracture control is mandatory for all crewed and critical space systems. In accordance with the American approach, composite structures are ranked according to the degree of fail-safety. For structures with redundant load paths, where the failure of one element does not lead to the loss of the entire system, the use of statistical basis B is permitted in determining the strength properties of the material (Raju et al., 2010). Basis B means that, with a 95% confidence level, no less than 90% of the material population will demonstrate properties above the design values. For unique load-bearing elements without redundancy, the more stringent basis A properties are applied, 95% confidence for 99% of the population (Raju et al., 2010). For composite shells, NASA-STD-5019A prescribes a strict survivability assessment procedure, DTA, while requiring that the structure withstand design ultimate loads even in the presence of manufacturing defects prior to launch.

The procedures by the European Space Agency are similar to those by NASA. The European Space Agency standard ECSS-E-ST-32-01C specifies the required use of Fail-Safe architecture in composite fairings as well as statistically based B-bases (Raju et al., 2010). The European standard is unique in that it requires a detailed evaluation of the risk of degradation due to exposure to impacts and that the analytical calculations should be supplemented with mandatory full-scale tests of ability to withstand internal pressure (Bogenfeld et al., 2024).

The Japan Aerospace Exploration Agency regulates fracture control for composites in the JERG-0-001F standard (JAXA, 2022). A specific feature of the JAXA approach is the requirement for analytical proof that microfluctuations in the structure will not grow to critical dimensions during the time calculated by the formula Life Requirements × 4. For composite shells, JAXA strictly requires confirmation of the LBB (Leak Before Burst) criterion, guaranteeing that fatigue-crack growth will lead to depressurization. In addition, for fiberglass composites, the Japanese standard requires mandatory assessment of strength under prolonged static loading, whereas for carbon-fiber-reinforced plastics, this analysis may be omitted. Table 1 presents a comparative analysis of the requirements of leading aerospace regulators for ensuring the Damage Tolerance of composite structures.

**Table 1. Comparative analysis of the requirements of leading aerospace regulators for ensuring the damage tolerance of composite structures**

| Feature / Regulator | NASA, USA | ESA, Europe | JAXA, Japan |
|---|---|---|---|
| Baseline Fracture Control standard | NASA-STD-5019A | ECSS-E-ST-32-01C | JERG-0-001F |
| Approach to statistical property | A-basis (Single-path), B-basis (Fail-Safe) | B-basis (Fail-Safe) | Statistical tolerances, 4× design life margin |

| | | | |
|---|---|---|---|
| bases for CFRP | | | |
| Primary criterion for composites | Demonstrated residual strength with defects | Demonstrated strength with defects + mandatory Proof Test | Mandatory Leak Before Burst, detailed Stress Rupture assessment |
| Allowance for macroscopic damage growth | Strictly limited due to lack of on-orbit repairs | Strictly limited, focus on impact damage | Allowed only within validated analytical life assessment |

The strategic transition to defect-tolerant design produces a dualistic effect. On the one hand, the Damage Tolerance concept makes it possible to abandon the incorporation of colossal empirical safety factors that were applied blindly. The use of fail-safe schemes and precise crack-growth modeling makes it possible to reduce the mass of a composite fairing by up to several tens of percent, which is critically important for RLVs (Bogenfeld et al., 2024). On the other hand, this approach dramatically complicates, makes more expensive, and lengthens the validation and certification process.

For the certification of RLVs according to Damage Tolerance standards, implementation of the Building Block Approach, BBA, is required (Kim et al., 2022). The process begins with the testing of hundreds of elementary coupon specimens for the statistical determination of A- and B-bases, proceeds to the study of joints with artificially introduced defects, Teflon inserts for simulation of delaminations, indenter impacts for the creation of BVID, and culminates in full-scale tests of fairing sections under stochastic cyclic loading (Raju et al., 2010). It is precisely for this reason that the development of accurate mathematical models capable of partially replacing physical experimentation within the BBA paradigm is of paramount importance to the industry.

## 1.3. Typology of Manufacturing Defects in PCMs

A fundamental ontological problem in the composite manufacturing of large-scale load-bearing structures, to which the monolithic halves of the payload fairings of reusable launch vehicles with diameters from 3 to 9 meters belong, is the technological impossibility of achieving a zero defect level (Fu & Yao, 2022). This is conditioned by the very nature of composite materials: unlike metallurgy, the formation of the part's final geometry and the synthesis of the material occur simultaneously, making the structure extremely sensitive to variations in technological parameters (Kalariya et al., 2023).

In the contemporary aerospace industry, fairings are formed predominantly by the Automated Fiber Placement method, AFP. The AFP method offers substantial advantages over traditional hand layup in terms of productivity and reproducibility (Kukwi et al., 2025). Nevertheless, the specificity of laying narrow prepreg tows onto surfaces of complex double curvature using robotic heads inevitably leads to technological anomalies. The introduction of zones of local thickness variation, reinforcement zones beneath mating frames, as well as the application of promising Out of Autoclave, OOA, technologies, exponentially increases the density and diversity of defects. Table 2 shows comparative defect statistics in the manufacturing of composite structures.

**Table 2. Comparative Statistics of Defects in Composite Structure Manufacturing: Automated Layup vs. Hand Layup (Coherent Market Insights, 2025; Space Foundation, 2025)**

| Quality metric | Hand Layup | Conventional AFP system | AFP with integrated AI + inspection/control |
|---|---|---|---|
| Defect rate | 5–15% | 3–5% | 0.8% |
| Coefficient of variation, material properties | >10% | 5–7% | <5% |
| Process capability index, Cpk | 0.8–1.0 - Low | 1.33–1.67, Acceptable | >2.0 High – Six Sigma |
| Quality inspection coverage | 10% Sampling inspection | 100% In-line, continuous | 100% + predictive analytics |

Delaminations and disbonds represent a violation of interlaminar adhesion interaction or the absence of bonding between the polymer skin and the honeycomb core. Their appearance is associated with the ingress of foreign inclusions, such as the prepreg protective film. The cause may also be insufficient or nonuniform pressure of the compacting roller of the AFP head. An additional factor is a nonuniform temperature gradient during curing. Under the action of vibroacoustic flexural loads, the edges of delaminations become pronounced concentrators of shear stresses. This creates conditions for the growth of a macrocrack.

Fiber waviness constitutes a geometric curvature of reinforcing fiber bundles in the plane of the ply or with out-of-plane deviation. In the AFP process, waviness systematically arises when prepreg is laid onto concave regions during steering. This is associated with excessive tension or with tow slippage. Such a defect sharply reduces the composite's compressive strength. Curved fibers lose longitudinal stability. Micro-buckling develops.

For this defect, the literature contains quite concrete estimates. It has been experimentally shown that, as the severity of waviness increases, compressive strength decreases almost linearly, and at a high defect severity of about 0.075, the strength reduction may reach 75% compared with defect-free material. For this reason, fiber waviness is regarded as one of the most dangerous defects in compression-loaded composite shells (Nair et al., 2017).

Gaps and overlaps are specific kinematic defects in robotic AFP layup. A gap occurs when adjacent tows do not close together. During polymerization, this volume is filled with epoxy binder. Resin-rich areas are formed. Such resin-rich areas serve as centers of microcrack initiation. An overlap occurs when tows run onto one another. This leads to local laminate thickening. Forced waviness is also formed in all overlying plies.

Porosity is the accumulation of microscopic gas voids within the polymer matrix. It arises as a consequence of air entrapment between tow layers during layup. Another cause is the release of volatile chemical fractions during the resin's exothermic polymerization. High porosity substantially reduces the matrix's shear modulus. This facilitates the development of interlaminar shear under the action of acoustic waves.

Quantitatively, this effect has been experimentally confirmed. Reviews on composites note that a void content above 1% already leads to noticeable degradation of interlaminar and flexural characteristics, and at a level of about 6.6%, the reduction in interlaminar shear strength may reach approximately 25% (Taheri et al., 2025). Consequently, even moderate porosity directly affects life in matrix-dominated loading regimes.

Recent deep statistical studies, including analyses of hundreds of batches of helicopter and rocket composite panels, have revealed a fundamental mechanical regularity. The presence of manufacturing defects radically transforms the statistical nature of material failure (Elhajjar, 2025).

Defect-free composites manufactured under laboratory conditions demonstrate a narrow, unimodal distribution of ultimate strength, usually well described by a Weibull distribution with a high shape parameter, with a coefficient of variation COV at the level of 3–4%, which is comparable to aerospace aluminum (Elhajjar, 2025). However, the injection of defects, such as porosity or fiber waviness, into the macrostructure transforms the failure probability density into a complex, multimodal distribution with distinctly pronounced heavy tails. The coefficient of variation in industrial composites rises to 15–20% (Elhajjar, 2025).

Mathematically, this phenomenon is explained by the concave shape of the function describing the relationship between normalized residual strength and a geometric defect parameter, such as the relative depth of a fiber wave. In accordance with a theorem of probability theory, Jensen’s inequality, for any strictly concave function, the mathematical expectation of the function of a random variable is always less than or equal to the function of its mathematical expectation (Elhajjar, 2025):

$$E[f(X)] \leq f(E[X]).$$

The Jensen Gap, resulting from defect dispersion, signifies a fundamental engineering problem: the presence of local random variations in defectiveness degrades the real load-bearing capacity of the structure disproportionately more than predicted by simplified models based on the mean defectiveness. This effect manifests itself with particular vividness under compression, where fiber waviness generates extreme statistical outliers in the left-hand part of the distribution. In these zones, the probability of premature shell failure, accompanied by a reduction in strength to 60% of the nominal value, exceeds by orders of magnitude the predictions calculated using the classical three-sigma rule (Elhajjar, 2025). Figure 8 shows the mechanism by which technological defects in automated layup influence the statistical transformation of the distribution of PCM strength.

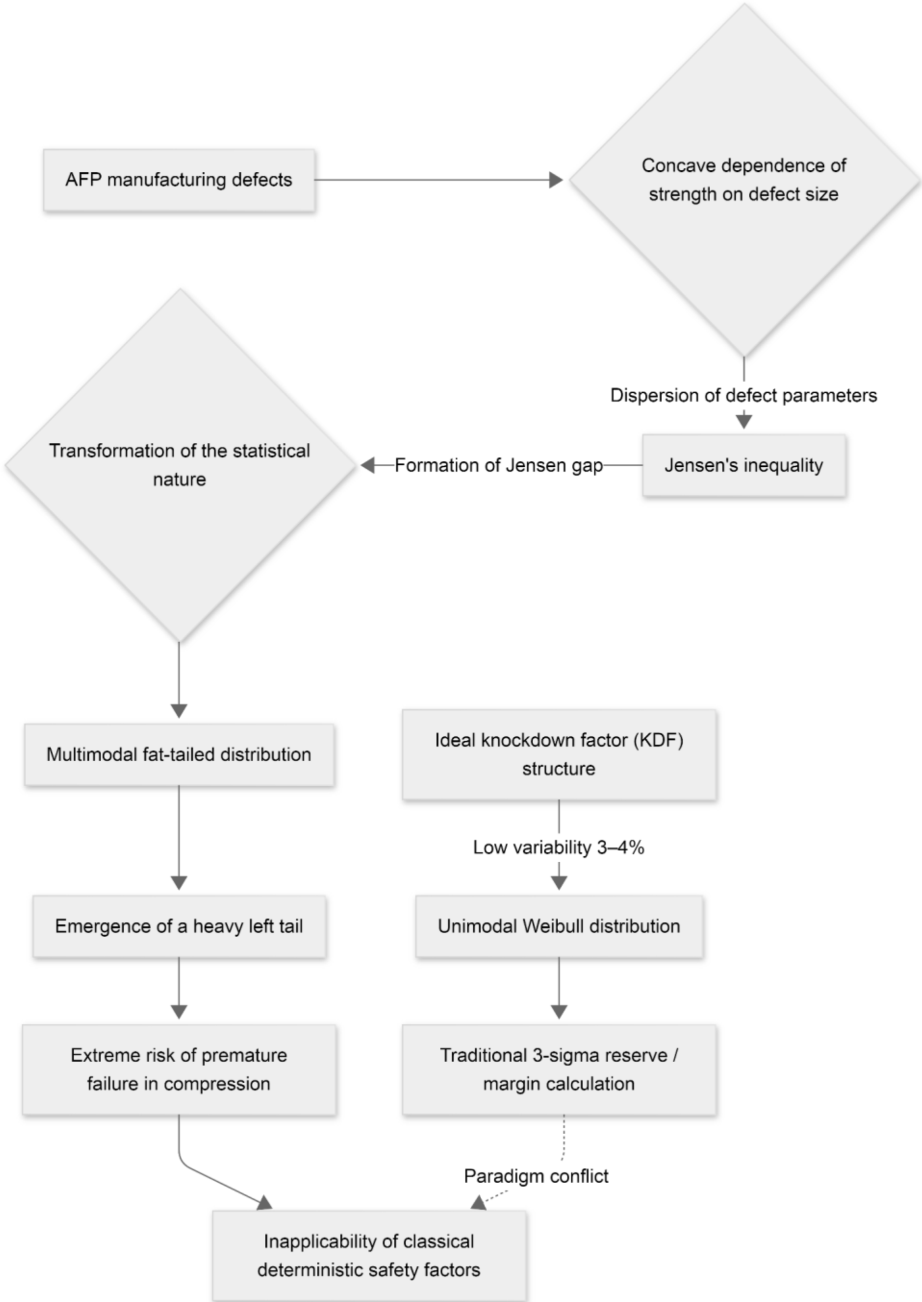


**Fig. 8.** The mechanism of influence of technological defects of automated layup on the statistical transformation of the distribution of the strength

Under conditions of vibroacoustic loading, when the external load itself is stochastic in character, the superposition of these two random fields, the stochasticity of loading, and the fat-tailed stochasticity of strength, renders the application of classical deterministic safety margins for reusable fairings inadmissible and technically hazardous. This imperatively requires a transition to stochastic fracture mechanics.

## 1.4. Overview of Fracture Mechanics Methods

In view of the multilayered, orthotropic, and profoundly heterogeneous microstructure of polymer composite materials, classical strength criteria, such as the von Mises, Tsai–Wu, or Hill criteria, which are oriented toward homogeneous isotropic bodies, exhibit extremely low predictive accuracy in the presence of initial macrodefects (Cao et al., 2025). The mathematical modeling of the kinetics of growth of inevitable technological defects, such as delaminations and microcracks, under the destructive action of stochastic vibroacoustic loads requires the mandatory use of a powerful specialized mathematical apparatus, Fracture Mechanics.

The basic analytical foundation is Linear Fracture Mechanics. Although LFM was historically developed by Griffith and Irwin to describe the brittle fracture of metals and glass, in recent decades its apparatus has been successfully extended to anisotropic and orthotropic continua (Yang et al., 2026). The fundamental distinction of the fracture mechanics of composites lies in the fact that the main crack in them almost never propagates normal to the vector of maximum principal stresses, as in metals (Fakoor et al., 2025). A crack in PCM is collinear with the structural axes and invariably follows the path of least energetic resistance, along the orientation of the reinforcing fibers, matrix cracking, or strictly along the interface between layers of differing layup, interlaminar separation, delamination.

For the formulation of the planar LFM problem in an orthotropic fairing plate, the stress tensor in a small neighborhood of the singularity, the crack tip, is described through the generalized Hooke's law, including the matrix of independent effective elastic constants, longitudinal elastic modulus, shear modulus, and Poisson's ratio (Ayatollahi et al., 2021). The intensity of the stress field in the prefracture zone is rigidly characterized by Stress Intensity Factors, SIF, for three fundamental modes: normal opening of the crack faces, in-plane transverse shear, and antiplane longitudinal shear (Guo et al., 2025).

The analytical computation of SIF in large-scale composite PF panels is impossible due to their complex geometry, curvature, and edge effects. In contemporary computational mechanics, for the precise determination of SIF, energetic approaches are integrated: the path-independent Cherepanov–Rice J-integral, based on the strain-energy-density tensor, and its dual thermodynamic form, the I*-integral, resting upon the principle of minimum complementary energy (Yang et al., 2026). The invariance of these integrals makes it possible to circumvent the zone of mathematical stress singularity directly at the crack tip and to determine SIF with high precision along the far contour of the finite elements.

Discrete stepwise modeling of the spatial propagation of cracks in classical FEM requires continuous local remeshing of the finite-element mesh as the crack tip moves. For multidimensional layered shells, this process becomes computationally inefficient and leads to loss of convergence.

To overcome this fundamental barrier, the eXtended Finite Element Method, XFEM, as well as its isogeometric variations, is being actively introduced into RLV design practice (Kulkarni & Lal, 2024). The basic philosophy of XFEM consists in the use of the partition-of-unity concept. Into the basis functions of the standard FEM nodes through which the crack passes, special enrichment functions are mathematically injected. The Heaviside function describes the physical discontinuity of displacements on the crack faces, whereas the asymptotic functions describe the stress singularity at its tip (Kulkarni & Lal, 2024). This allows the crack to propagate through finite elements in a completely arbitrary manner, without reference to mesh boundaries.

However, for the modeling of the specific growth of interlaminar delaminations under the action of cyclic flexural vibroacoustic oscillations, the gold standard of the aerospace industry has become the Virtual Crack Closure Technique, VCCT, often applied in symbiosis with Cohesive Zone Models, CZM (Liu et al., 2023). The VCCT method rests upon Irwin's principle, which states that the energy released when a crack is increased by an infinitesimal amount $\Delta a$ is strictly equal to the work that must be performed by the applied external forces for the virtual forced closure of that crack over the same length. VCCT enables efficient computation of the strain-energy release rate and comparison with the composite's critical fracture toughness, automatically resolving the problem of delamination-front advancement without remeshing. Table 3 presents a comparative analysis of contemporary numerical methods of computational fracture mechanics for orthotropic layered fairing structures.

**Table 3. Comparative analysis of modern numerical methods of computational fracture mechanics for orthotropic layered structures of fairings**

| Evaluation criterion / Method | Classical FEM | Extended FEM | Virtual Crack Closure Technique |
|---|---|---|---|
| **Crack growth mechanics** | Strictly along existing finite-element boundaries | Arbitrary path through elements | Strictly along a predefined ply interface / layer boundary |
| **Need for remeshing** | Required at each local increment step of crack advance | Not required, uses nodal enrichment functions | Not required, uses a node-release algorithm |
| **Typical use in composite shells** | Global stress–strain state, stress analysis, resonance mode search for a payload fairing | Modeling intralaminar macrocracks and perforation / penetration | Modeling interlaminar delaminations |
| **Computational complexity** | Medium | Very high, complex integration of enriched elements | High, requires a fine mesh in the cohesive / crack-tip region |
| **Integration with fracture mechanics** | Basic integration with a separate/independent J-integral | Built-in mathematical stress singularity representation | Direct computation of energy release rate (G) |

The accumulation of structural damage in the fairing is purely random, initiated by broadband acoustic noise. The macroscopic development of a crack or delamination area is traditionally modeled using Paris' empirical differential equation, which describes the incremental increase in crack length per loading cycle, or its modifications for composites based on energy-release rates (Deng et al., 2023).

However, under the realities of vibroacoustic loading, the amplitude of flexural stresses in each cycle, and, as a direct consequence, the range of the stress intensity factor, is not a constant. It is a random variable obeying, for example, a Rayleigh distribution in the case of a narrow-band random process. Solving the stated problem requires a profound synthesis of the apparatus of fracture mechanics with the methods of probability theory, a transition to Stochastic Fracture Mechanics (Shi et al., 2025). The assessment of residual strength and the computation of failure probability for a composite PF panel are based on the formation of a multidimensional integral distribution function of the SIF, which must account for three sources of uncertainty. The statistical dispersion of the effective physico-mechanical properties of the PCM itself, fluctuations of stiffness matrices and elastic modulus from batch to batch, the random nature of the dimensions, geometry, and spatial orientation of initial technological defects relative to the principal axes of orthotropy of the shell, and the Power Spectral Density, PSD, of the stochastic external vibroacoustic excitation.

A particularly critical role in the Damage Tolerance concept is played by determining the initial defect size from which the integration of Paris' equation begins. This quantity cannot be chosen arbitrarily. It is rigidly determined by the capabilities of the applied nondestructive evaluation methods, such as phased-array ultrasonic testing (Ding et al., 2023). The statistical reliability of NDE is described by Probability of Detection, POD, curves. In the aerospace industry, two principal mathematical approaches to POD calculation are used: the method that yields a quantitative signal correlated with defect size, and the binary hit/miss method (Tai et al., 2024). According to the strict regulatory requirements of NASA-STD-5009C, nondestructive evaluation methods and personnel are obliged to demonstrate detection of a critical defect with a probability of 90% at a statistical confidence level of 95% (Parker et al., 2023). The integration of POD curves into stochastic XFEM calculations is the cornerstone of forming a reliable prediction of the residual life of an RLV.

Only the comprehensive, synergistic application of stochastic extended FEM and probabilistic Markov-type algorithms enables reliable calculation of the kinetics of degradation in the residual strength of a composite material in each cycle of broadband spectral loading. Figure 9 presents a conceptual algorithm for integrating NDE methods, hybrid vibroacoustic analysis, and stochastic fracture mechanics for assessing the residual life of PCM.

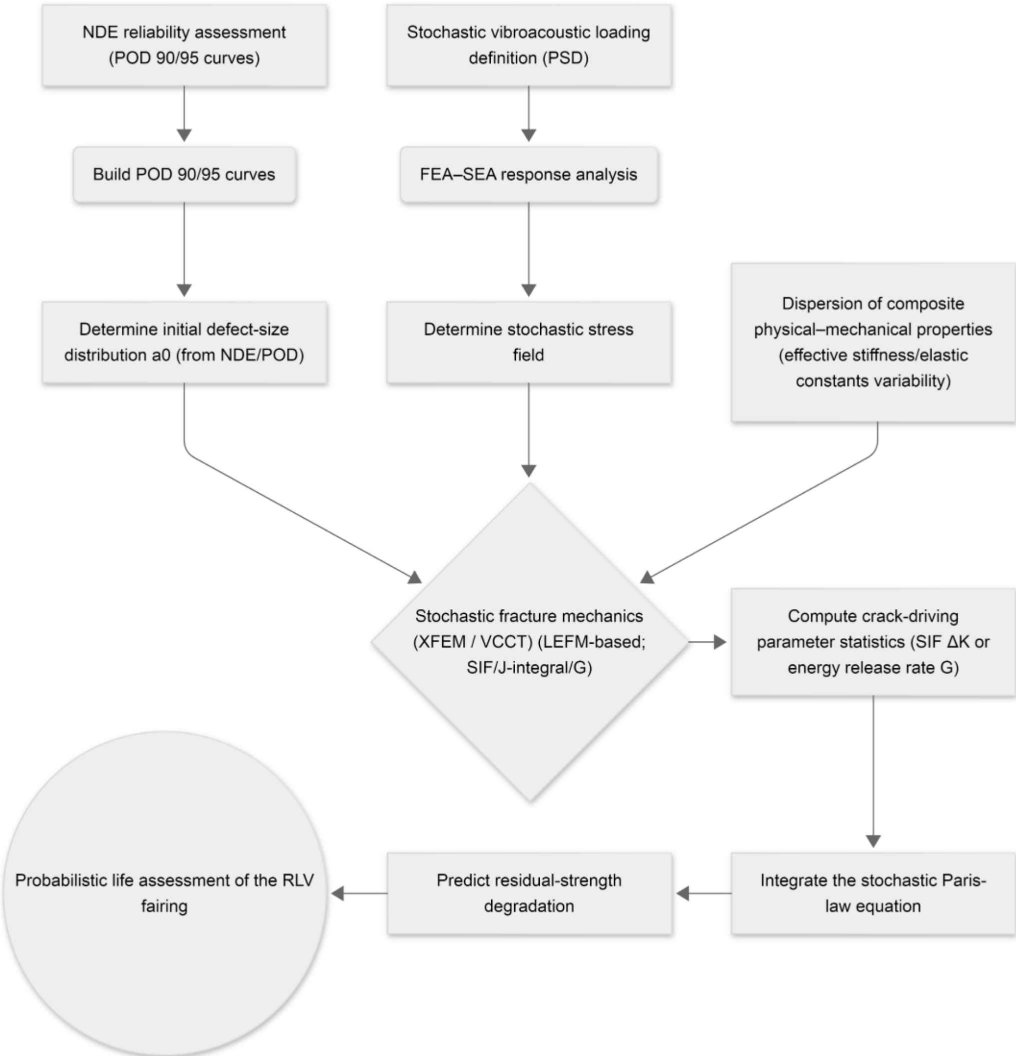


**Fig. 9.** A conceptual algorithm for integrating NDE, hybrid vibroacoustic analysis, and stochastic fracture mechanics methods for assessing the residual life

Thus, to ensure the operational reliability of composite fairings on reusable launch vehicles, there arises an absolute scientific-engineering necessity for the development of a unified, comprehensive, interdisciplinary hybrid model, Acoustics + Crack. This conceptual model must seamlessly integrate methods of statistical energy analysis. This is needed for the adequate reconstruction of the high-frequency diffuse acoustic spectrum and for the extended finite-element method for the precise local calculation of stress intensity factors in an orthotropic heterogeneous medium. Also, the apparatus of stochastic fracture mechanics with the integration of the probability of defect detection, for predicting the kinetics of degradation of the residual life of PCM at all stages of RLV operation.

# CHAPTER 2.
# Modeling of the Vibroacoustic Response of the Structure

The design process for reusable launch vehicles requires a fundamentally different approach to dynamic strength analysis compared with traditional expendable systems. If the principal task for expendable products is to ensure integrity during a single flight cycle, then for RLVs, understanding the mechanisms of damage accumulation under repeated high-intensity loads becomes critically important (Calabuig et al., 2024). Within the structure of these loads, vibroacoustic effects arising at the launch stage and during passage through regions of maximum aerodynamic pressure are dominant. This chapter presents a methodology for modeling vibroacoustic response, integrating mathematical models of random pressure fields, numerical methods of modal-characteristic analysis, and calculations of the stress-strain state of layered shells.

For clarity and continuity, the practical calculations presented in Chapters 2–4 are illustrated using a representative structural segment of a reusable launch vehicle's payload fairing. The reference case corresponds to a local region of the cylindrical section located in the vicinity of a circumferential frame, where elevated vibroacoustic stresses are expected. The laminate thickness is assumed to be 3.2 mm. Nondestructive inspection is assumed to identify an initial interlaminar delamination with a characteristic length of $a_0$ = 8 mm. For the structural zone under consideration, the operational defect limit is set at 16 mm, while the critical defect size is assumed to be 20 mm. Unless stated otherwise, this reference case is used in the subsequent sections to demonstrate the practical application of the proposed methodology.

## 2.1. Mathematical Model of Acoustic Excitation

During launch, the acoustic field acting on the launch vehicle skin is a stochastic phenomenon, which is due to the turbulent mixing of the main engine jet plume with the surrounding free stream (Escartí-Guillem et al., 2023). In terms of engineering modeling, such excitation can be approximated by the Diffuse Sound Field concept. The DSF model assumes a spatially homogenous sound energy at the structural surface and an isotropic pressure field (Zotter et al., 2024).

The mathematical formalization of such a field requires the apparatus of the theory of random functions. The principal characteristic of the excitation in the frequency domain is the Power Spectral Density, PSD, of pressure fluctuations $S_{pp}(\omega)$, describing the distribution of sound intensity over the frequency spectrum. The relationship between pressure at two spatially separated points of the surface is determined through the Cross-Power Spectral Density, CPSD, function. For an ideal diffuse field in three-dimensional space, the spatial correlation function is formulated as following:

$$G_{p1p2}(r,\omega) = S_{pp}(\omega)\frac{sin(kr)}{kr},$$

where $k = \omega/c$ is the wave number, $r$ is the distance between the points, $c$ is the speed of sound in the medium, $\omega$ is an angular frequency. This dependence is key to forming the load-matrix in finite-element models. For real launches, however, the field is not perfectly diffuse, and the launch structure, flame trenches, rocket surface, etc., also add distortions to the initially correlated field, resulting in patches of correlation depending on the directionality of the radiation from the jet plume (Escartí-Guillem et al. 2024).

For model refinement during transonic flight and at the Max-Q, maximum dynamic pressure condition, the apparatus for turbulent-boundary-layer modeling is applied. In this regime, the pressure spectrum shifts toward higher frequencies, and spatial correlation begins to depend on the convection velocity of vortical structures (Dróżdż et al., 2023).

The engineering implementation of the acoustic-excitation model in contemporary software packages is based on the method of superposition of uncorrelated plane waves. The structural surface is divided into segments, to each of which an ensemble of random loads is applied, whose phase and amplitude components are generated by the Monte Carlo method so as to correspond to the prescribed coherence function (Van hoorickx & Reynders, 2022). Such an approach enables high-precision simulation of the excitation of a broad spectrum of the fairing shell's natural modes.

An important aspect is the consideration of the Acoustic Fill Effect, arising because of the interaction of the external field with the internal volume of the fairing, within which the payload is placed. The presence of the satellite alters the modal density of the air cavity, leading to local pressure amplifications at frequencies corresponding to the acoustic resonances of the gap between the shell and the spacecraft. The process of acoustic loading of the payload fairing during launch is shown in Figure 10.

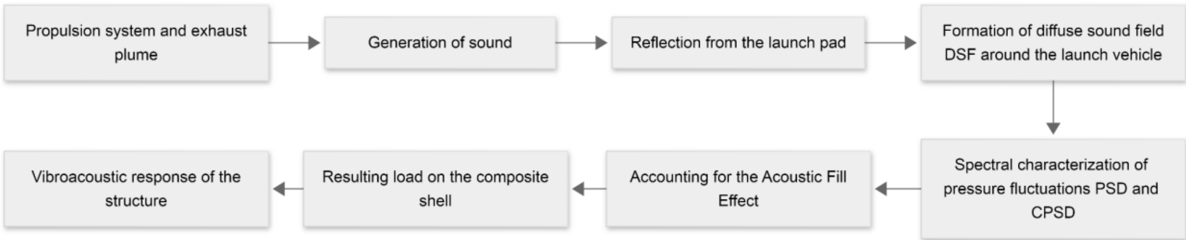


**Fig. 10.** The process of forming the acoustic loading of the payload fairing at the launch stage

## 2.2. Numerical Analysis of the Natural Frequencies and Mode Shapes of the Fairing

The determination of the dynamic characteristics of large-scale composite shells is a complex computational problem that requires consideration of material orthotropy and the geometric specifics of the fairing. The fairing consists of a conical, i.e., nose, and cylindrical section that create geometric discontinuities. The finite element numerical analysis was carried out using high-performance finite element codes (Mishra et al., 2023) .

The modal analysis is based on the solution of a generalized eigenvalue problem for the conservative system:

$$([K] - \omega^2[M])\{\phi\} = 0$$

where $[K]$ is the stiffness matrix, $[M]$ is the mass matrix, $\omega$ are the natural frequencies, and $\{\phi\}$ are the natural mode shapes. For composite structures, the matrix $[K]$ is formed by summing the contributions of each layer while accounting for its orientation and elastic constants in the local coordinate system (Kaddaha et al., 2021).

The significance of the choice of layer orientation is additionally confirmed by the very range of properties of the reinforcing material. For contemporary carbon fibers, the elastic modulus may vary from approximately 40–200 GPa for low-modulus classes up to 600–950 GPa for ultra-high-modulus classes, whereas strength lies in the range of approximately 1–7 GPa depending on the fiber class. This means that even with the same shell geometry, variation in the composition and orientation of the reinforcement can noticeably shift the natural frequencies and alter the modal density of the structure (Alam et al., 2019).

In the modeling of carbon-fiber fairings, it is critically important to use shell elements that account for transverse shear deformations, such as Mindlin–Reissner theory or higher-order theories, since neglecting them leads to an overestimation of stiffness and, consequently, to an error in frequency determination (Sayyad et al., 2022). According to contemporary studies, to ensure convergence in vibroacoustic problems, it is necessary to maintain a finite-element mesh density of at least 6–10 elements per flexural wavelength at the maximum analysis frequency (Li et al., 2024).

Of special interest is the analysis of the influence of manufacturing defects on modal characteristics. The presence of delamination zones leads to a local reduction in flexural stiffness, which manifests as splitting of natural frequencies or the appearance of specific mode shapes associated with the opening of the defect faces. The principal types of modal forms characteristic of composite payload fairings and their influence on structural reliability are presented in Table 4.

**Table 4. Main modal characteristics of a composite payload fairing and their impact on structural reliability**

| Modal characteristic | Description for composite payload fairing | Impact on reliability |
|---|---|---|
| Lowest bending modes | Global bending of the launch vehicle as an integrated structure | Additional loads on the flight control system |
| Shell modes | Radial pulsations of the cylindrical section | Peak dynamic stresses in the composite material |
| Ring frequency | Bending wavelength becomes equal to the circumference of the shell | Sharp increase in sound radiation and vibration transmission |
| Coincidence frequency | Bending wave speed equals the speed of sound in air | Maximum acoustic energy transmission into the interior |

Numerical experiments show that varying ply-layup angles in the PCM stack enables purposeful alteration of modal density in critical frequency ranges (Shonkwiler et al., 2023). This opens the possibility of detuning the structure from resonances driven by engine acoustics. However, for reusable systems, this optimization must account for stiffness degradation over the life cycle. A flowchart of the finite-element modal analysis process for a composite shell is shown in Figure 11.

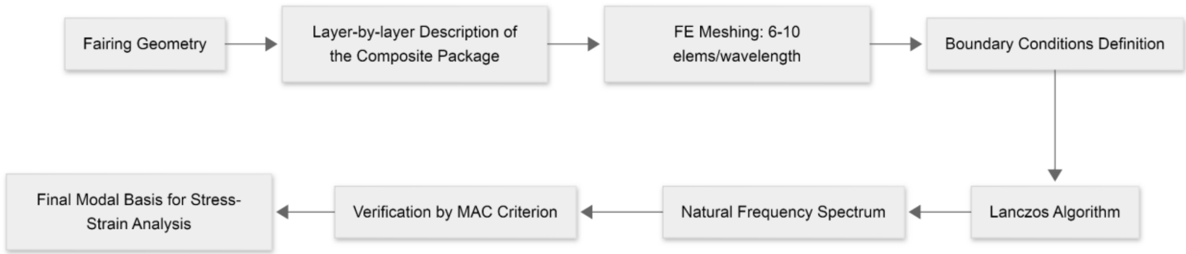


**Fig. 11.** Flow chart of the finite element modal analysis process for a composite shell

## 2.3. Calculation of the Stress-Strain State of the Shell

After the modal basis is formed, forced-vibration analysis is performed under a stochastic acoustic field. In engineering applications it is normal to use the Random Vibration Analysis method when the loading is assumed to be stationary and ergodic (Chiarelli, 2025). The objective is to find the dynamic-stress fields for each layer of the composite stack, as dynamic stresses are the main factor in fatigue degradation.

The stress spectral density matrix is computed by transforming the input pressure PSD through the stress transfer functions:

$$[S_\sigma(\omega)] = [H_{\sigma p}(\omega)][S_p(\omega)][H_{\sigma p}(\omega)]^{*T}$$

where $[S_\sigma(\omega)]$ is the stress spectral density matrix, $[S_p(\omega)]$ is the pressure PSD matrix, $[H_{\sigma p}(\omega)]$ is the matrix of transfer functions from pressure to stresses, $*$T denotes complex-conjugate transposition. The resulting Root Mean Square stresses $\sigma_{rms}$ are obtained by integrating the PSD over frequency:

$$\sigma_{rms} = \sqrt{\int_{f_{min}}^{f_{max}} S_{\sigma\sigma}(f)df},$$

where $f$ is frequency, and $S_{\sigma\sigma}(f)$ is the autospectral density of stress.

For the reference fairing segment introduced above, consider the following illustrative calculation. Assume that integration of the stress power spectral density over the frequency range from 20 to 400 Hz yields

$$\int_{20}^{400} S_{\sigma\sigma}(f)df = 324\ MPa^2.$$

The resulting root mean square stress is therefore

$$\sigma_{rms} = \sqrt{324} = 18\ MPa.$$

If one assumes, for a stationary Gaussian random process, that potentially dangerous local peak stresses may reach approximately $3\sigma_{rms}$, then the expected peak stress becomes

$$\sigma_{max} = 3 \times 18 = 54\ MPa$$

If the allowable local stress for the structural zone under consideration is set to 60 MPa, the resulting margin with respect to peak stress amplitudes becomes critically small. This example demonstrates that even moderate RMS stress levels can produce peak stress excursions that approach or exceed allowable limits under stochastic vibroacoustic excitation, thereby creating conditions favorable for the initiation of damage and subsequent crack development in composite structures.

For composite fairings, stress-strain analysis reveals several zones of extreme dynamic stress concentration. First and foremost, these are regions near technological openings and hatches, where complex biaxial states arise. Under acoustic resonance, local stresses in these zones may exceed nominal shell values severalfold. Of particular danger are interlaminar shear stresses, since it is precisely these that are responsible for the growth of hidden delaminations under the action of flexural waves.

Probabilistic methods such as the Jensen Gap may also account for random scatter based on ply thickness or defects in lay-up on the local stress-strain state (Gao et al., 2020). Statistics also show that even a small amount of porosity can cause a large change in the stress redistribution to the stiffer plies, and thus accelerate their premature failure (Tavaf & Banerjee, 2022). Stress concentration zones in composite-metal structures and their stress-strain behavior are summarized in Table 5.

**Table 5. Stress Concentration Zones in Composite-Metal Structures and Their Stress-Strain Behavior**

| Structural zone | Cause of stress concentration | Nature of the stress-strain state |
|---|---|---|
| Butt joint frame | Abrupt CFRP–metal stiffness mismatch | High interlaminar shear stresses |
| Ply-drop zones | Geometric singularity at the step transitions | Through-thickness peeling normal stresses |
| Vicinity of holes | Interruption of load-carrying fibers | Tensile/compressive stress concentration |
| Sandwich core | Skin vibration over honeycomb cells | Core crushing and shear |

Stress-strain-state calculation must also account for thermal action at the Max-Q stage. Aerodynamic heating reduces the elastic modulus of the polymer matrix, which leads to softening of the shell, reduction of its natural frequencies, and, as a consequence, alteration of resonant regimes and stress amplitudes. The algorithm for calculating the dynamic stress-strain state of the composite fairing shell is shown in Figure 12.

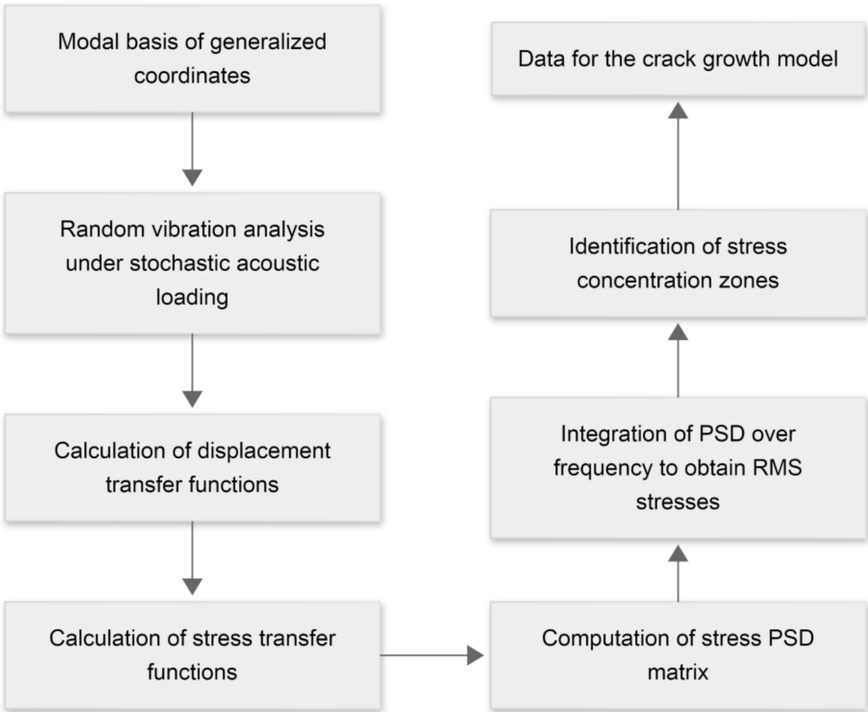


**Fig. 12.** Algorithm for calculating the dynamic stress-strain state of the composite fairing shell

## 2.4. Verification of Numerical Models

As shown in Chapter 1, given the high level of responsibility for RLV structures, verification and validation of vibroacoustic models is a mandatory stage regulated by NASA and ESA standards. The principal objective of verification is to confirm that the selected numerical algorithms and discretization parameters adequately describe the process's physics.

In contemporary RLV design practice, results obtained in different software packages are cross-compared. A leader in the field of structural dynamic analysis is MSC Nastran, whereas ANSYS Mechanical is often used for the detailed analysis of nonlinear effects and multiphysical interaction (Pelekis et al., 2025). Comparative analysis shows that, for identical finite-element meshes, the differences in natural frequencies between these packages are less than 1%, which testifies to the high reliability of the basic solvers (Towner & Band, 2012).

However, the principal difficulties arise in modeling the interaction between the structure–acoustic medium. For verification, data from full-scale Reverberant Acoustic Tests, RAT, are used. During such tests, the fairing is subjected to a diffuse field with a prescribed spectrum, and the response is recorded by a network of accelerometers and strain gauges (Wang et al., 2024).

At the stage of subsequent inspection of critical zones, the quantitative sensitivity of control methods is likewise already well known. For phased array ultrasonic testing, it has been shown that defects of about 0.8 mm in size can be detected at composite-structure thicknesses up to 25 mm, and owing to the better signal-to-noise ratio and lower jitter level, the real sensitivity may be even higher than in conventional single-element UT (Taheri & Hassen, 2019). This is especially important for composite fairing panels, where small defects must be tracked before they progress to the accelerated-growth stage. Figure 13 shows that, at a specimen thickness of 25 mm and an artificial-hole diameter of 0.8 mm, the PAUT response exhibits a more distinct reflection from the defect and the back wall than conventional SEUT, confirming its higher practical detectability in small-damage monitoring tasks.

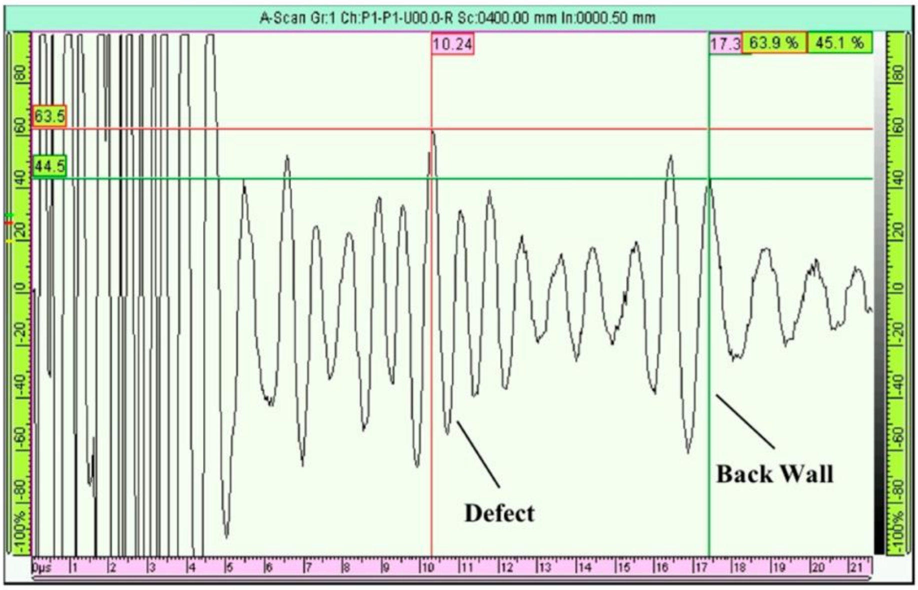


a)

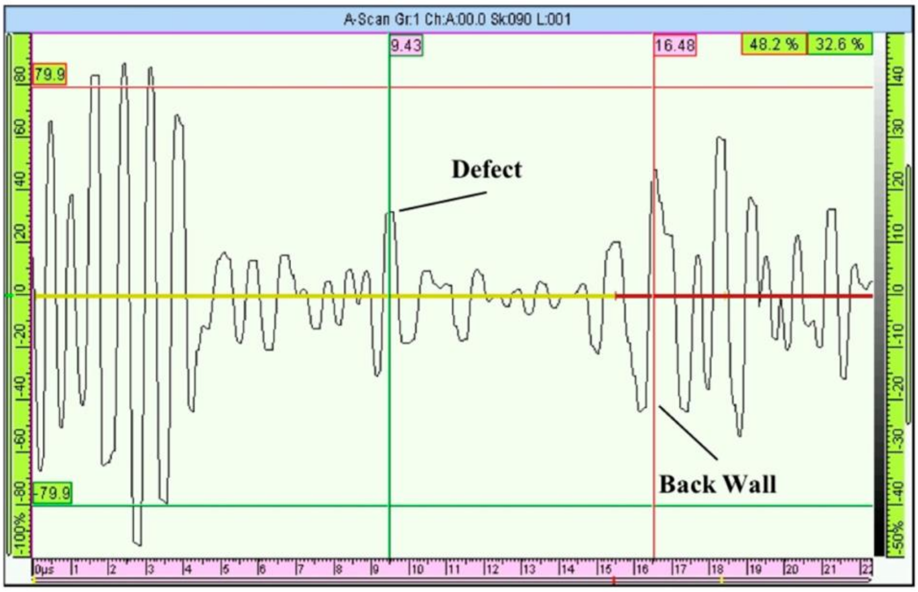


b)

**Fig. 13.** Comparison of SEUT (a) and PAUT (b) responses when detecting an artificial defect with a diameter of 0.8 mm in a GFRP specimen with a thickness of 25 mm (Taheri & Hassen, 2019)

Special attention is devoted to the choice of the damping model. In PCM, damping is complex and depends on frequency, amplitude, and temperature (Murčinková et al., 2022). Using a simplified damping coefficient can lead to significant errors in peak resonant stresses. A more accurate approach is to use experimentally obtained modal damping for specific layup types. The scheme of the vibroacoustic model validation and verification process is shown in Figure 14.

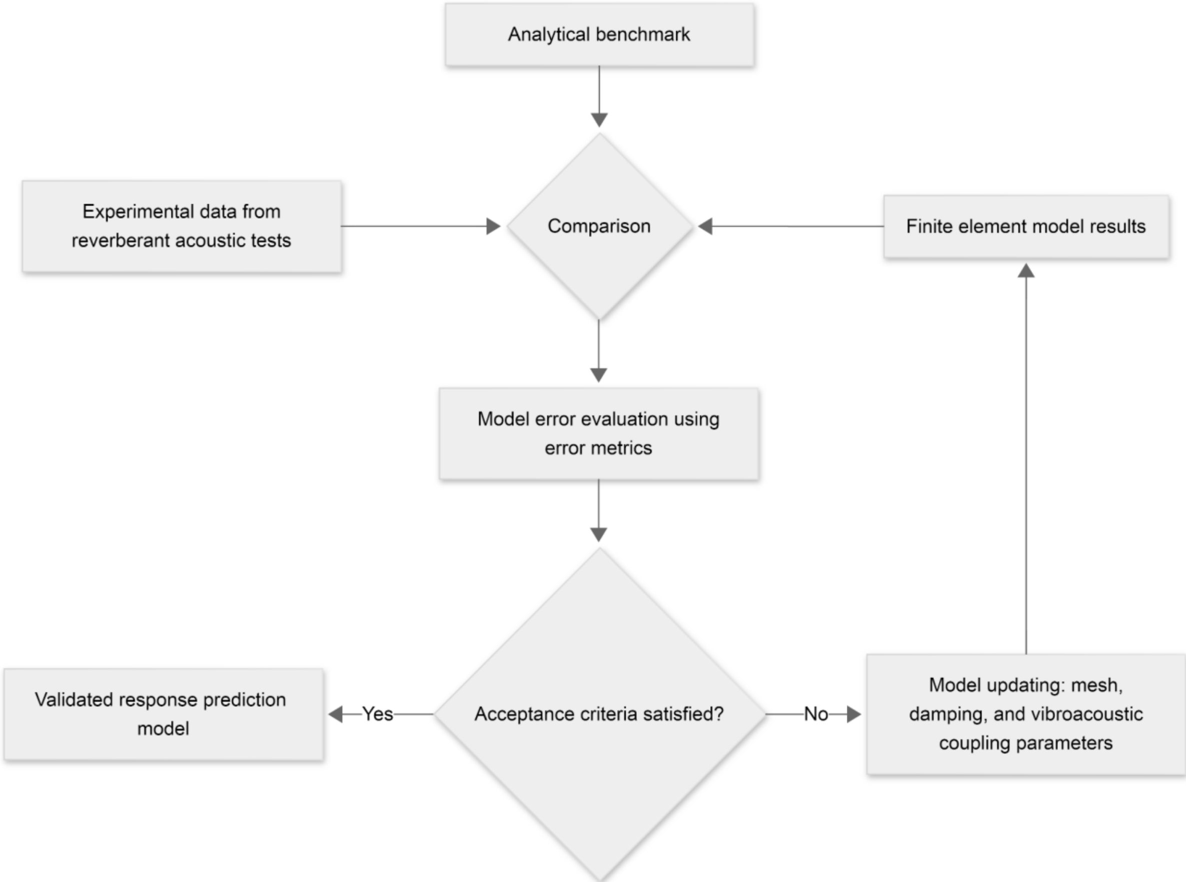


**Fig. 14.** Scheme of the process of validation and verification of the vibroacoustic model

In comparing ANSYS and MSC Nastran, two levels of the problem should be distinguished. At the level of the structure proper, both packages rest upon mature finite-element solvers and, with a consistent mesh, usually yield close modal characteristics. The difference manifests itself in the shift in computational emphasis. MSC Nastran is traditionally convenient for basic linear dynamics, modal analysis, random response, and serial computational verification. ANSYS provides a broader, more technologically coherent set of tools for a coupled formulation when shell vibrations are considered jointly with pressure in the surrounding or internal gas cavity. In the contemporary literature, it is precisely such a coupled formulation that is regarded as necessary for a reliable description of the vibroacoustic response of thin-walled composite systems (Dash et al., 2025). It is emphasized separately that accuracy in this problem is determined by the method used to discretize the acoustic domain and by the quality of the description of the coupling at the media interface.

If the approaches to modeling the acoustic medium are compared directly, ANSYS is more convenient for problems that require an expanded description of the medium itself (Ansys, n.d.). Its formulations include a diffuse-sound-field model under random excitation, models of porous and viscothermal media, and matched and one-way schemes for coupling the medium to the structure. This is useful when it is necessary to approximate the calculation to reverberation-chamber conditions or to account for absorbing and transition layers. In MSC Nastran, the line of calculation, based on proven schemes for coupled and uncoupled acoustic analysis, frequency response, and modal characteristics of the coupled system, is more clearly expressed. Such a path is especially convenient for cross-verification of frequencies, mode shapes, and the structure's integral response. Experimental studies on panel–cavity type systems show that reliable verification should rest simultaneously on two groups of measurements, structural accelerations and sound pressure in the cavity, since it is precisely their joint processing that makes it possible to reliably reconstruct the natural frequencies and damping coefficients of the coupled system (Liu et al., 2022).

From an engineering perspective, the final comparison is formulated as follows. MSC Nastran is well-suited as a reference computational benchmark for linear vibroacoustic verification, whereas ANSYS is well-suited as a more flexible environment for refining local effects, especially in zones of complex coupling between the structure and the acoustic domain, and in problems where medium properties and damping influence response peaks. Such a two-package approach makes it possible to proceed from comparison of frequencies and pressures to the principal result, the fields of dynamic stresses in critical plies, joints, and cutouts. It is precisely these fields that subsequently serve as the initial loading basis for assessing damage accumulation and ensuing crack growth. Contemporary works on the vibroacoustics of composite systems show that refinement of damping and correct description of the structure–medium coupling noticeably alter modal-energy distribution, acoustic-response levels, and, consequently, the extreme stresses upon which the durability margin depends (Dash et al., 2025).

## 2.5. Engineering Significance of the Obtained Results

The results of modeling the fairing's vibroacoustic response obtained within the framework of this chapter form the foundation for strategic engineering decisions in the creation of reusable systems. The engineering significance of these data extends far beyond formal confirmation of strength and encompasses economics, safety, and RLV certification.

First, the identification of zones of dynamic-stress concentration and the determination of their spectral characteristics are critically important for implementing the Damage Tolerance concept. The obtained stress fields serve as input data for fracture-mechanics models, allowing prediction of the growth rate of technological defects during operation. This makes it possible to scientifically substantiate the in-flight life of the structure and determine optimal intervals of nondestructive evaluation.

Second, a detailed understanding of the modal response enables deep optimization of the fairing's weight efficiency. Abandoning excessive deterministic safety margins in favor of probabilistic calculations that account for the actual load spectrum enables reducing the structure's passive mass. In the economics of RLV, every kilogram of dry mass saved is converted into additional payload or fuel savings during the first-stage return.

Third, the modeling results enable targeted measures to protect the payload. Analysis of the internal acoustic field and the Fill effect enables optimization of the placement and characteristics of acoustic mats or metamaterials, minimizing their mass while preserving the required level of noise reduction. Engineering Implications of the Obtained Results for RLV Design are shown in Table 6.

**Table 6. Engineering Implications for RLV Design**

| Application area of results | Practical impact for RLV | System-level significance |
|---|---|---|
| Fracture mechanics | Prediction of the remaining service life of PCM | Safety of multiple launches |
| Mass optimization | Reduction in the dry mass of the liquid oxygen tank | Increased cost-effectiveness |
| Non-destructive testing | Focus of NDE on critical zones | Reduced maintenance time |
| Certification | Mathematical proof of survivability | Faster flight clearance |

Finally, the creation of a digital twin of the vibroacoustic response is a necessary condition for the transition to predictive analytics of the condition of the launch-vehicle fleet. The comparison of flight-telemetry data with the results of numerical models in real time makes it possible to detect in timely fashion anomalous structural behavior associated with latent damage development, which constitutes the apex of contemporary engineering thought in the field of aerospace reliability. The influence of simulation results on the operational strategy of reusable systems is shown in Figure 15.

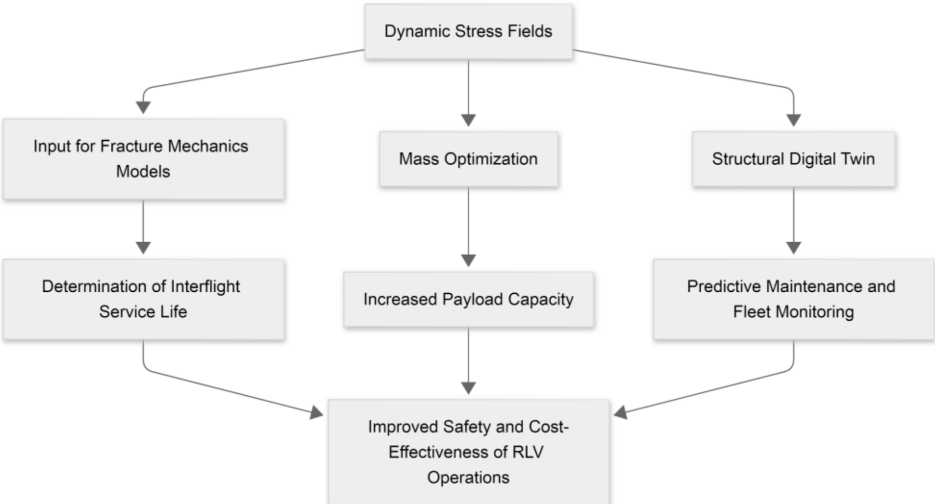


**Fig. 15.** Impact of simulation results on the operational strategy of reusable systems

Thus, Chapter 2 forms an analytical bridge between the stochastic nature of the external environment and the physics of damage accumulation in the material. The presented modeling methodologies enable the safe execution of current missions and lay the foundation for the next generation of ultra-reliable, economically efficient reusable space transportation systems.

# CHAPTER 3.
# Fracture Mechanics and Crack Growth Modeling in Orthotropic Media

As substantiated in the preceding chapters, the incorporation of polymer composite materials into the architecture of highly loaded assemblies of reusable space transportation systems is driven by their outstanding specific strength. However, the layered, heterogeneous, and orthotropic nature of these materials gives rise to specific degradation mechanisms that differ radically from the fatigue behavior of traditional isotropic metallic alloys. Under the action of high-intensity stochastic vibroacoustic loads generated during launch and passage through the zone of maximum aerodynamic pressure, inevitable technological macrodefects, for example, interlaminar delaminations, porosity, or disbonded regions, become capable of unpredictable growth. This chapter formulates a methodology for computational fracture mechanics that integrates advanced spatial discretization methods, energetic criteria for assessing the fracture toughness of orthotropic media, and stochastic algorithms for predicting fatigue crack growth. The analytical instruments presented herein serve as the basis for transitioning from the conservative Safe-Life concept to probabilistic design under Reliability-Based Damage Tolerance.

## 3.1. FEM Specificities in Fracture Mechanics Problems

The central problem in computational mechanics for assessing the residual strength of aerospace structures is the correct mathematical modeling of singular stress and strain fields in the local vicinity of the tip of a macroscopic defect. In linear elastic fracture mechanics, stresses at the crack tip tend to infinity. In Chapter 2, it was shown that the components of the stress tensor increase inversely proportionally to the square root of the polar distance from the crack front.

The traditional finite element method, based on standard polynomial shape functions (linear or quadratic), is not capable of accurately representing the singular stress gradient at the crack tip without extremely fine mesh refinement, which becomes computationally prohibitive for large-scale structures. As a result, classical FEM approaches alone are insufficient for reliable fracture analysis in composite aerospace systems.

To overcome the limitations of classical FEM, specialized discretization approaches have been developed to accurately represent stress singularities in the vicinity of defects. Early engineering solutions were based on geometric distortion of finite elements to reproduce the asymptotic stress field near crack tips. Among these, the most established and reliable method is the use of singular isoparametric elements, which are widely implemented in commercial CAE systems such as Abaqus and Nastran (Dinkler et al., 2024). These elements enable accurate local representation of fracture behavior without requiring excessive global mesh refinement.

The essence of this method is the deliberate displacement of the intermediate nodes of a standard 8-node planar or 20-node spatial quadratic element by a distance equal to one quarter of the element's side length from the crack tip (Saouma & Amin, 2021).

Mathematically, this operation distorts the Jacobian $[J]$ of the coordinate transformation from the global Cartesian system $(x, y)$ to the local isoparametric system $(\xi, \eta)$. The coordinate transformation function $x$ along the side of the element takes the form of a nonlinear polynomial whose roots generate the required singularity. Since strains are computed through the inverse Jacobian $[J]^{-1}$, shifting the intermediate node to the L/4 position leads to the determinant of the Jacobian tending to zero at the crack tip when $\xi = -1$, naturally forming a root-type strain and stress gradient $r^{-1/2}$, precisely corresponding to the analytical solutions of LEFM.

For the modeling of cracks in PCM, around the mathematical point of the tip a specialized local mesh, a rosette, is formed. It is created by collapsing one of the faces of a quadratic element into a point. The nodes of the collapsed face are assigned independent degrees of freedom, which allow the element to open and adequately describe the physical blunting of the tip and the opening of the crack faces Crack Opening Displacement, COD, in a layered orthotropic medium. A comparative analysis of finite element methods for crack modeling in PCM is presented in Table 7.

**Table 7. Comparative analysis of finite element methods for modeling cracks**

| Method characteristic | Traditional FEM | Singular elements | Extended FEM | Cohesive Zone Method |
|---|---|---|---|---|
| **Mathematical basis** | Taylor polynomials | Jacobian distortion | Partition of Unity | Traction-Separation model |
| **Singularity modeling** | Impossible, approximation only | Exact reproduction | Incorporation of asymptotic functions | Absent, resolved by the zone physics |
| **Mesh topology requirements** | Extremely fine mesh | Conforming mesh, rosette around the crack tip | Mesh is independent of crack geometry | Elements are inserted between composite laminate plies |
| **Defect growth modeling** | Full remeshing required | Rosette reconstruction at each step | Free growth through elements | Growth strictly along the layer interface |
| **Optimal application in RLV** | Global stress-strain state of the fairing | Static analysis | Skin penetration, complex fracture path | Interlaminar delamination |

Despite the high accuracy of singular elements, in modeling stochastic fatigue crack growth under random vibroacoustic loads, the need for constant local remeshing along the moving fracture front renders the calculations inefficient. For orthotropic multilayer shells, this process is associated with the risk of convergence loss. The solution is the Extended Finite Element Method, XFEM, the application of which to gradient and orthotropic materials has been actively investigated in recent years (Vellwock & Libonati, 2024).

XFEM is based on the Partition of Unity concept, enabling the enrichment of the standard polynomial approximation space with local discontinuous and singular functions without altering the topology of the underlying mesh (Vellwock & Libonati, 2024). The approximation of the displacement field $U_h(x)$ for an element intersected by a crack is written as:

$$U_h(x) = \sum_{i=1}^{N_{enr}} N_i(x)u_i + \sum_{j=1}^{N_d} N_j(x)H(x)a_j + \sum_{k=1}^{N_t} N_k(x) \sum_{\alpha=1}^{4} F_\alpha(x) b_k^\alpha$$

where $N_i(x)$ are the standard shape functions of node i; $u_i$ are the classical nodal degrees of freedom, displacements; $H(x)$ is the modified Heaviside function taking the values +1 or -1 on opposite sides of the crack surface, describing the physical discontinuity of the continuum, i.e., a strong discontinuity; $a_j$ are the additional degrees of freedom for nodes whose elements are completely cut by the crack; $F_\alpha(x)$ are the enrichment functions of the crack tip, describing the asymptotic singular stress field; $b_k^\alpha$ are the additional degrees of freedom for nodes containing the crack front; $U_h(x)$ is the approximated displacement field at point $x$; $N_d$ is the number of nodes enriched by the Heaviside function; $N_t$ is the number of nodes enriched by the crack-tip functions; $\alpha$ is the number of the enrichment function at the crack tip; i, j, k denote the nodal sets over which summation is performed.

A fundamental distinction in the application of XFEM to PCM lies in the structure of the enrichment functions. Whereas for isotropic metals simple trigonometric functions of the half-angle are used, for orthotropic composites the functions must strictly satisfy the conditions of anisotropic elasticity theory. They are derived from the Lekhnitskii–Stroh complex potentials and depend on the roots of the characteristic equation of the material, taking into account the direction of the reinforcing fibers relative to the crack plane. The algorithm for selecting and integrating finite element strategies for the discretization of macrodefects in the RLV composite fairing is shown in Figure 16.

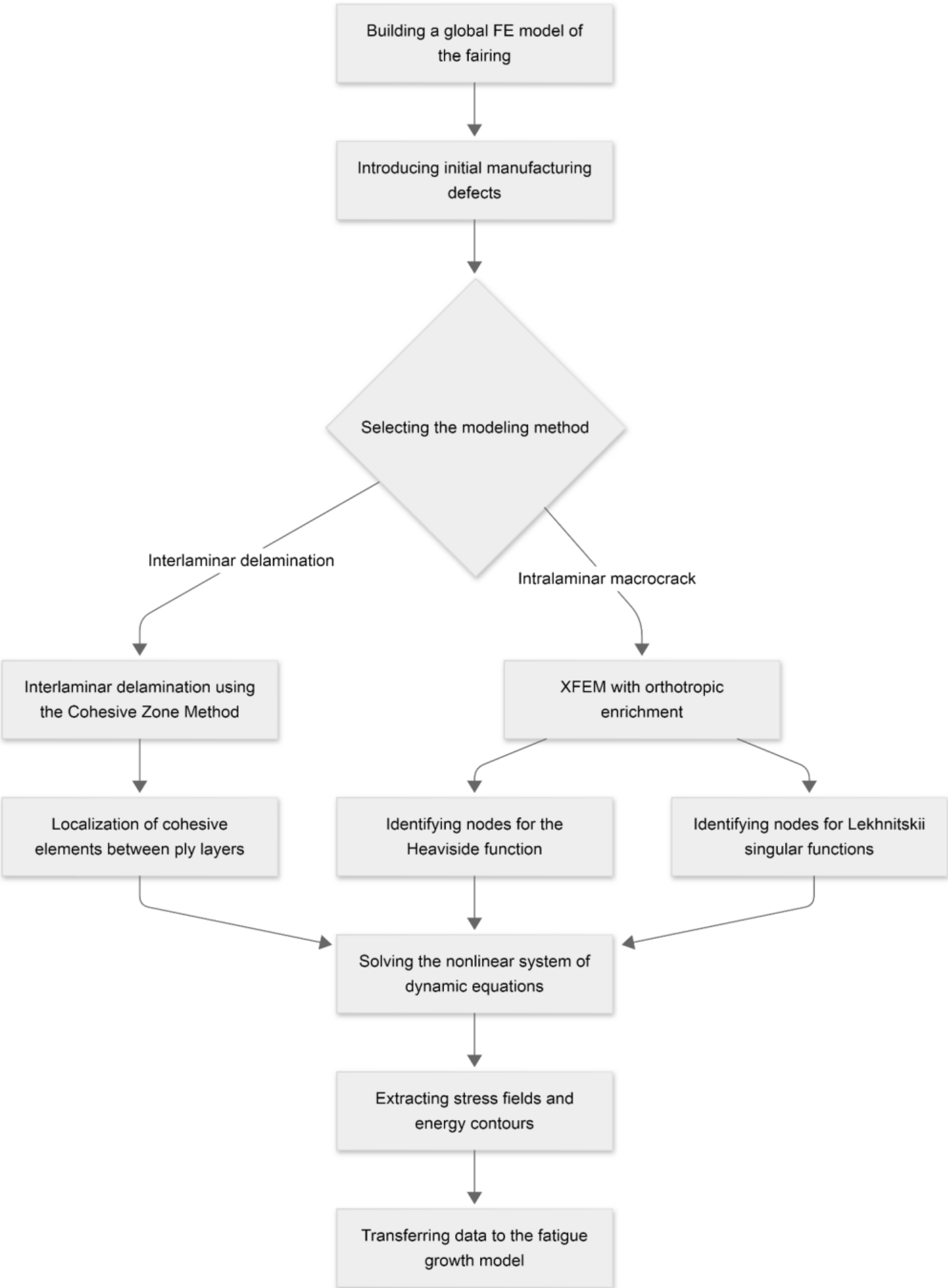


**Fig. 16.** Algorithm for selecting and integrating finite element strategies for discretizing macrodefects in the RLV composite fairing

Modeling within XFEM requires integrating a specialized mathematical apparatus for tracking the moving crack geometry. For this purpose, the Level Set Method, LSM, is used. Two orthogonal functions $\phi(x)$ and $\psi(x)$ make it possible to determine with high precision the position of the crack body and its front at any moment in time, automatically activating additional degrees of freedom as the defect advances under vibroacoustic fatigue.

## 3.2. Calculation of Stress Intensity Factors

The stress field in the small vicinity of a singularity is rigidly characterized by the Stress Intensity Factor, SIF. SIF is a dimensional scalar quantity, MPa*m$^{1/2}$, completely determining the stress state at the defect tip within the framework of LEFM.

For homogeneous isotropic materials, for example, aluminum alloys 2024-T3, historically used in rocketry, the solutions of Griffith, Irwin, and Isida provide exact analytical relationships (Bi et al., 2024). In an idealized infinite plate, the opening-mode SIF is determined as $K_I = \sigma\sqrt{\pi l}$. In real structures, such as fairing panels of finite width *B*, a correction factor Y is introduced, accounting for the influence of geometric boundaries: $K_I = \sigma\sqrt{\pi l} \cdot Y(\lambda)$, where $\lambda = l/B$.

In composite structures, calculating SIF becomes more complicated owing to the pronounced anisotropy of the stiffness and compliance matrices. In contrast to isotropic media, where fracture modes (I - opening, II - longitudinal shear, III - transverse shear) are independent, in orthotropic layered plates, strong mode mixing arises. Normal opening stresses may induce shear deformations, and vice versa.

The analytical and semi-analytical determination of stresses in the vicinity of the crack tip in a composite is based upon the Lekhnitskii–Stroh formalism (Hwu & Becker, 2022). For the state of plane stress, the characteristic equation of anisotropic elasticity theory is written through the coefficients of the compliance matrix $a_{ij}$:

$$a_{11}\mu^4 - 2a_{16}\mu^3 + (2a_{12} + a_{66})\mu^2 - 2a_{26}\mu + a_{22} = 0.$$

The roots of this equation $\mu_k$ $(k = 1,2)$ are pairwise complex conjugates. Physically, they reflect the degree of anisotropy of the material and determine the spatial distribution of stresses. The displacement vector $U_i(r,\theta)$ and the stress tensor $\sigma_{ij}(r,\theta)$ are expressed through the Lekhnitskii matrices $A_{ik}$ and $B_{kj}$:

$$U_i(r,\theta) = \sqrt{2r/\pi} \cdot Re\left[\sum_{k=1}^{2} A_{ik} \cdot \sqrt{Z_k(\theta,\mu_k)} \cdot B_{kj} \cdot K_j\right]$$

where $Z_k(\theta,\mu_k) = cos\theta + \mu_k sin\theta$, and the vector $K_j = [K_I, K_{II}]^T$. This mathematical structure shows that, in PCM, SIF depends on the crack geometry and the applied load, as well as on the material's elastic constants and the crack orientation relative to the principal symmetry axes of orthotropy.

The orientation of reinforcing carbon fibers $\theta$ relative to the defect-propagation plane exerts a critical influences fracture kinetics. Under the action of stochastic vibroacoustic loads on the payload fairing, the shell experiences complex bending and membrane deformations.

Experimental and numerical studies show that the degree of anisotropy, the modulus ratio $E_1/E_2$, and the angle $\theta$ radically alter the local SIF values (Abbasi et al., 2024). If a crack is initiated in the polymer matrix and propagates parallel to the fibers, i.e., $\theta = 0°$, it encounters minimal resistance, which leads to rapid intralaminar cracking.

However, when the front of a main crack reaches a ply whose fibers are oriented at 90° or 45° to the growth direction, a fundamental mechanism of arrest and trajectory change arises. The fibers act as a mechanical barrier. Local stresses are redistributed, initiating the bridging process, unbroken fibers connect the crack faces behind the crack front, generating closing, compressive forces that mathematically reduce the effective SIF range at the tip itself.

Moreover, because of the fibers' high tensile strength, it is energetically more favorable for the macrocrack to change direction. A deflection of the fracture plane occurs: an intralaminar crack transforms into an interlaminar delamination that propagates along the interface between layers of differing orientation. Thus, quasi-isotropic and hybrid layups are deliberately used in the design of RLV fairings to redirect fracture energy and prevent through-thickness perforation of the shell. Table 8 shows the influence of reinforcing-fiber orientation on the local stress-strain state and the mechanisms of fracture mechanics.

**Table 8. The influence of the orientation of reinforcing fibers on local stress-strain state and mechanisms of fracture mechanics**

| Fiber Orientation Relative to the Crack Front | Effect on the Local Stress Field | Characteristic Change in SIF | Main Dissipation and Failure Mechanism |
|---|---|---|---|
| **0°, Parallel** | No structural barriers. The stress field is concentrated in the brittle matrix. | Sharp increase in $K_I$. $K_{II}$ is minimal. | Intralaminar longitudinal matrix cracking. |
| **90°, Perpendicular** | Fibers intersect the singularity zone. A gradient of compressive forces develops behind the crack front. | Significant local reduction in $K_I$, shielding effect. | Crack arrest, fiber bridging, fiber breakage. |
| **±45°, Angled lay-up** | Redistribution of normal stresses into shear stresses. | Activation of mixed-mode fracture, increase in $K_{II}$ and $K_{III}$. | Crack kinking, shear-driven matrix failure. |
| **Quasi-isotropic hybrid lay-up** | Global stiffness equalization, but formation of high interlaminar shear stresses. | Complex $K_I/K_{II}$ balance. Oscillation of the singularity. | Energy transfer into interlaminar delamination onset. |

Direct computation of SIF via stress extrapolation in FEM for layered composites is prone to high errors due to the oscillatory nature of stresses at layer interfaces. Therefore, contemporary computational practice is based upon invariant energetic criteria.

## 3.3. Energetic Fracture Criteria

The fundamental thermodynamic criterion of fracture mechanics is the Strain Energy Release Rate, SERR, denoted as $G$. According to the Griffith–Irwin energetic concept, a crack begins to grow when the elastic strain energy $G$, released upon an increase in crack area by an infinitesimal amount $da$, reaches the critical value - the material fracture toughness $G_c$ (Chaudhari et al., 2021). In composite structures subjected to flexural vibroacoustic oscillations, the dominant and most dangerous degradation mechanism is interlaminar delamination, the growth of which strictly obeys energetic laws.

For the computation of $G$ in complex spatial structures, the path-independent Cherepanov–Rice J-integral is used. For a two-dimensional problem, it expresses the law of energy conservation on the contour $S$, surrounding the crack tip:

$$J = \int_s \left(W\delta_{1j} - \sigma_{ij}\frac{\partial u_i}{\partial x_1}\right) n_j ds,$$

where $W = \frac{1}{2}\sigma_{ij}\epsilon_{ij}$ is the density of potential elastic strain energy, $u_i$ are the components of the displacement vector, and $n_j$ are the components of the outward normal vector to the integration contour. Within the framework of LEFM for elastic materials, the strict identity $J = G$. A characteristic feature of the J-integral is that the integration contour may be taken far beyond the zone of stress singularity, into the region of large, regular finite elements, which ensures outstanding accuracy in numerical calculations.

However, the classical J-integral possesses a fundamental drawback for composite structures: it computes only the total energy release rate $G_{Total}$. For layered PCM, the critical fracture toughness in normal opening $G_{Ic}$ may be an order of magnitude lower than the fracture toughness in longitudinal shear $G_{IIc}$. The action of an acoustic wave on an RLV fairing generates a complex mixed stress state, which requires strict decomposition of the total energy into the components $G_I, G_{II}$ and $G_{III}$.

To perform mode decomposition, the Interaction Integral Method, also known as the M-integral, is used (Lv et al., 2018). This method is based on the principle of superposition: the actual stress field calculated in FEM is combined with the mathematically prescribed auxiliary Lekhnitskii–Stroh field. The total J-integral for the superposed state is equal to:

$$J^{(act+aux)} = J^{(act)} + J^{(aux)} + M^{(1,2)}.$$

The interaction integral $M^{(1,2)}$ takes the form:

$$M^{(1,2)} = \int_s \left(W^{(act,aux)}\delta_{1j} - \sigma_{ij}^{(act)}u_{i,1}^{(aux)} - \sigma_{ij}^{(aux)}u_{i,1}^{(act)}\right) n_j ds.$$

By assigning unit SIF values in the auxiliary field, for example, $K_I^{(aux)} = 1, K_{II}^{(aux)} = 0$, the actual value $K_I$ for the orthotropic structure can be algebraically extracted through the computed value of $M^{(1,2)}$ and then converted into $G_I$. An analogous procedure is performed for $G_{II}$. This method is implemented in the computational core of XFEM modules of contemporary CAE packages.

For the modeling of the kinetics of interlaminar delaminations along a known contact plane, the gold standard in aerospace design has become the Virtual Crack Closure Technique, VCCT (Liu et al., 2023). The method is based upon Irwin's thermodynamic principle, stating that the energy released when the crack grows by $\Delta a$, is mathematically equivalent to the work of external and internal forces required to forcibly close the crack faces over the same length.

The advantage of VCCT lies in the direct extraction of the components of the energy release rate directly from nodal forces and displacements in a single FEM calculation step. For a 2D finite element model, the components $G$ are computed by the formulas:

$$G_I = \frac{1}{2B\Delta a} F_{y,i}\Delta v_{i-1}, G_{II} = \frac{1}{2B\Delta a} F_{x,i}\Delta u_{i-1},$$

where $F_{y,i}, F_{x,i}$ are the components of nodal reactions at the crack tip, node $i$; $\Delta u_{i-1}, \Delta v_{i-1}$ are the relative mutual displacements of the crack faces in nodes $i-1$, located immediately behind the front; $B$ is the element width.

For the reference fairing segment introduced above, consider the following illustrative example of an interlaminar delamination assessment. Let the finite element width be $B = 25\,mm = 0.025\,m$, and let the virtual crack extension increment be $a = 1\,mm =$

$0.001\, m$. Assume that the finite element solution provides the following nodal forces and relative crack-face displacements:

$$F_y = 180\, N, \quad v = 0.04\, mm = 4 \times 10^{-5}\, m,$$
$$F_x = 260\, N, \quad u = 0.06\, mm = 6 \times 10^{-5}\, m.$$

Then the mode-I component of the strain energy release rate is

$$G_I = \frac{(180 \times 4 \times 10^{-5})}{(2 \times 0.025 \times 0.001)} = 144\, J/m^2,$$

whereas the mode-II component is

$$G_{II} = \frac{(260 \times 6 \times 10^{-5})}{(2 \times 0.025 \times 0.001)} = 312\ J/m^2.$$

Accordingly, the total strain energy release rate is

$$G_T = G_I + G_{II} = 456\, J/m^2$$

If the mixed-mode critical fracture toughness of the laminate is taken as $G_c = 454\, J/m^2$, then the condition $G_T > G_C$ is satisfied. Hence, under the assumed loading conditions, further propagation of the interlaminar delamination is expected to occur.

The assessment of crack stability and the condition for its advancement to the next element under mixed loading are determined by phenomenological criteria. The most accurate criterion for epoxy-matrix composites is recognized as the Benzeggagh–Kenane criterion (Babaevskiy et al., 2024):

$$G_c(\psi) = G_{Ic} + (G_{IIc} - G_{Ic}) \left(\frac{G_{II}}{G_T}\right)^{\eta},$$

where $G_T = G_I + G_{II}$ is the total energy, $\psi$ is the mode-mixity angle, $\eta$ is an experimentally determined material parameter. If the computed value $G_T$ exceeds the threshold value $G_c(\psi)$, the VCCT algorithm automatically breaks the connection between the nodes, simulating delamination growth. Figure 17 presents the operating logic of the VCCT algorithm in assessing the growth of interlayer delaminations under quasi-static and dynamic loads.

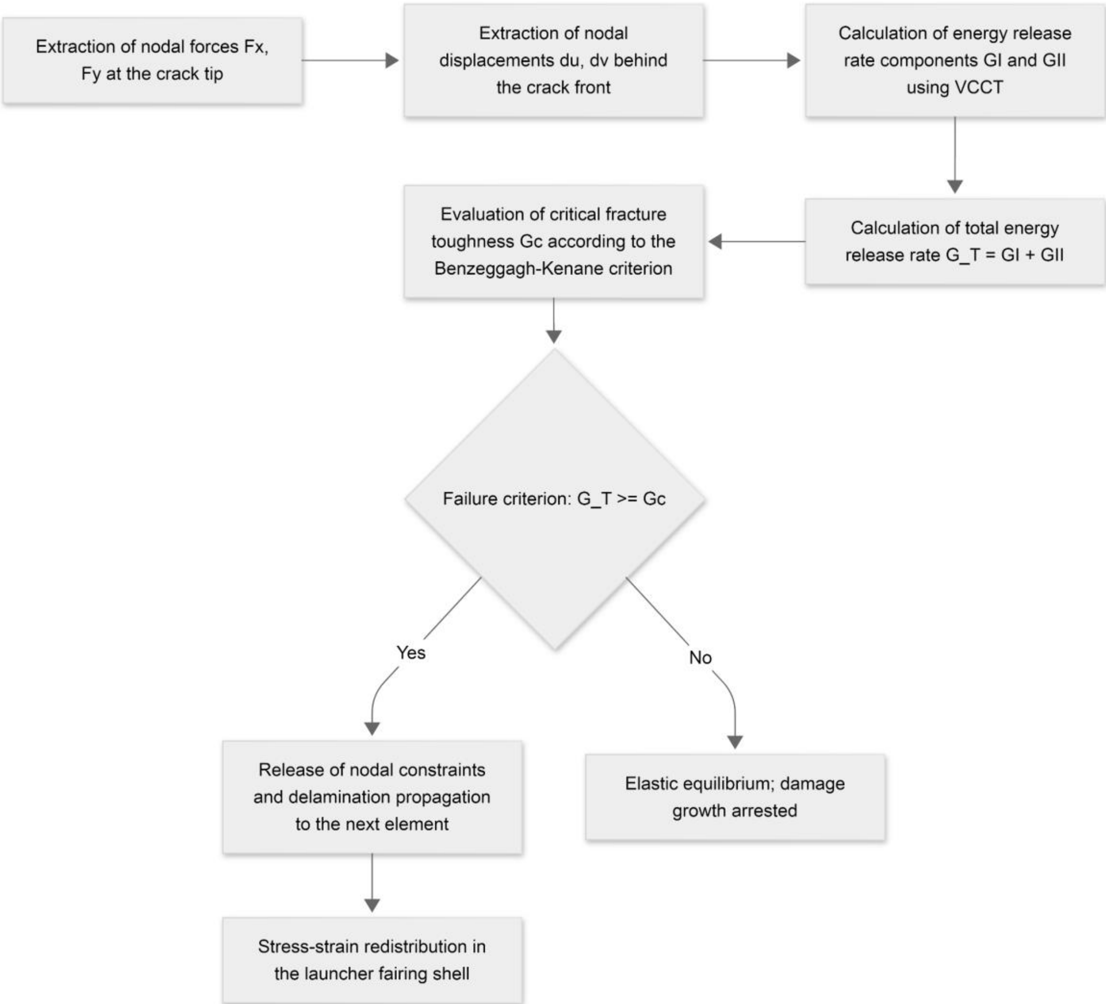


**Fig. 17.** The logic of the VCCT algorithm in assessing the growth of interlayer delaminations under quasi-static and dynamic loads

## 3.4. Fatigue Growth Modeling

The assessment of residual strength and survivability of an RLV payload fairing requires the integration of static energetic criteria with the laws of fatigue-fracture kinetics. The specificity lies in the fact that the acoustic action of the jet plume and the turbulent boundary layer forms a stochastic broadband vibrational response of the structure. Stress amplitudes in each cycle are random and form a spectrum close to a Gaussian distribution in the frequency domain.

Direct step-by-step integration of differential crack-growth equations in the time domain using Rainflow cycle-counting algorithms for acoustic frequencies requires analyzing hundreds of millions of cycles, rendering the problem computationally intractable at the conceptual design stage.

For linear systems, this is precisely why fatigue calculations based on PSD in the frequency domain are regarded as fundamentally more efficient: comparative studies note that they may be orders of magnitude faster than time-domain analysis involving direct generation of random signals followed by rainflow counting. Among spectral methods, the Dirlik and Tovo–Benasciutti approaches have become most widespread, and in comparative studies and experimental validations, the Dirlik method often demonstrates the most reliable agreement with rainflow-based estimates for broadband processes (Dirlik & Benasciutti, 2021).

The contemporary paradigm is stochastic modeling of fatigue crack growth in the frequency domain. This approach transforms the power spectral density PSD matrix of stresses or SERR, obtained from the hybrid FE-SEA model in Chapter 2, directly into the probabilistic distribution of cycle amplitudes.

The foundation of the method is the computation of the spectral moments $m_i$ of the function PSD $G(f)$:

$$m_i = \int_0^\infty f^i G(f) df.$$

The spectral moments contain exhaustive statistical information on the variance, central frequency, and the expected zero-crossing rate, $\upsilon_0 = \sqrt{m_2/m_0}$, and the peak rate $\upsilon_p = \sqrt{m_4/m_2}$.

To transform the PSD into the probability density function of the amplitudes of full stress cycles $p(S)$ Dirlik's empirical formula is used, which demonstrates the best convergence with Rainflow-analysis results for broadband processes (Gümüş et al., 2021). Dirlik's distribution is a superposition of one exponential and two Rayleigh distributions:

$$p(S) = \frac{1}{2\sqrt{m_0}}\left[\frac{D_1}{Q} exp\left(-\frac{Z}{Q}\right) + \frac{D_2 Z}{R^2} exp\left(-\frac{Z^2}{2R^2}\right) + D_3 Z exp\left(-\frac{Z^2}{2}\right)\right],$$

where $Z = S/(2\sqrt{m_0})$ is the normalized stress amplitude, and the dimensionless coefficients $D_1, D_2, D_3, R, Q$ are functions of the process-irregularity coefficient $\gamma = m_2/\sqrt{m_0 m_4}$. Dirlik's method makes it possible to assess with high accuracy the probability of occurrence of high-amplitude stress outliers, which make the dominant contribution to the initiation and growth of a fatigue crack.

The rate of macroscopic delamination propagation in a composite is traditionally described by the phenomenological Paris–Erdogan differential equation (Deng et al., 2023). In contrast to metals, where the SIF range is used, for polymer composites the equation is formulated through the range of the energy release rate. Dirlik's method makes it possible to assess with high accuracy the probability of occurrence of high-amplitude stress outliers, which make the dominant contribution to the initiation and growth of a fatigue crack.

The rate of macroscopic delamination propagation in a composite is traditionally described by the phenomenological Paris–Erdogan differential equation (Deng et al., 2023). In contrast to metals, where the SIF range is used, for polymer composites the equation is formulated through the range of the energy release rate $\Delta G = G_{max} - G_{min}$, or through $G_{max}$ at a given asymmetry ratio *R*:

$$\frac{da}{dN} = c_3(\Delta G)^{c_4},$$

where $\frac{da}{dN}$ is the increment of crack length per loading cycle, and $c_3, c_4$ are empirical material constants depending on mode mixity and temperature.

For the reference fairing segment introduced above, the Paris-type relation may be illustrated by a simple numerical example. Let a calibrated material-specific law be written in the form

$$\frac{da}{dN} = 2 \times 10^{-12}(\Delta G)^3,$$

where $\frac{da}{dN}$ is expressed in mm/cycle and $\Delta G$ is given in $J/m^2$. Assume that the equivalent energy release rate obtained from the local vibroacoustic response analysis is

$$\Delta G = 300\, J/m^2.$$

Then the crack growth rate becomes

$$\frac{da}{dN} = 2 \times 10^{-12} \times 300^3 = 5.4 \times 10^{-5}\, mm/cycle.$$

If one launch is assumed to correspond to 20,000 damage-relevant loading cycles, the delamination increment per launch is

$$\Delta a_{launch} = 5.4 \times 10^{-5} \times 20{,}000 = 1.08\, mm.$$

Accordingly, an interlaminar defect with an initial length of 8 mm may be expected to grow by approximately 1 mm per launch under the assumed loading scenario.

To assess the expected mean crack-growth rate $E[da/dt]$ under random stationary vibroacoustic loading, integration of the modified Paris law with Dirlik's probability density function is performed:

$$E\left[\frac{da}{dt}\right] = \upsilon_p \int_0^{\infty} \quad c_3\left(\Delta G_{eq}(S)\right)^{c_4} p(S)dS,$$

where $\Delta G_{eq}(S)$ is the equivalent strain energy generated by a stress cycle of amplitude $S$.

For more precise prediction of crack kinetics, especially in the near-threshold region and the avalanche-like fracture regime, the nonlinear NASGRO equation is used (Maierhofer et al., 2014). The NASGRO model accounts for local crack closure, which is critically important under random vibrations, where frequent low-amplitude cycles may not cause defect growth due to residual compressive stresses in the plastic zone ahead of the crack front.

Integration of the probability distribution function, PDF, with kinetic equations makes it possible to implement a stepwise algorithm: at each increment $\Delta t$ of flight time, the defect-length increment $\Delta a$ is computed, after which the geometry of the FE model is updated through XFEM or VCCT, the stiffness matrix is corrected, and the spectral response is recalculated.

## 3.5. Engineering Significance of the Obtained Results

The developed methodology for computing energetic contours and stochastic modeling of fatigue kinetics extends beyond purely theoretical computational mechanics and establishes a practical engineering framework for predicting structural reliability under realistic operating conditions. These results possess direct applied significance, providing a technologically grounded basis for implementing the Damage Tolerance concept in reusable space transportation systems, where accurate prediction of defect evolution and residual life is essential for ensuring both safety and economic efficiency.

In classical rocketry of expendable systems, the concept of safe life was applied, based on enormous empirically unjustified safety factors introduced blindly to compensate for manufacturing defects (Hoole et al., 2020). Under the economic model of RLV, where every kilogram of dry airframe mass is converted into payload loss and reduced profitability, such an approach is unacceptable.

For composites, this practice is especially inadequate, because their fatigue failure is not reducible to the growth of a single dominant crack, as is often modeled for metallic parts. Reviews on CFRP fatigue directly emphasize that, under cyclic loading, matrix microcracks, fiber breaks, debonding along the fiber–matrix interface, and interlaminar delaminations all develop simultaneously within the material. Thus, the problem of the life of a composite shell is an ensemble of interacting damage mechanisms (Alam et al., 2019).

According to contemporary strict regulatory requirements, space regulators require composite airframe structures of RLVs to be certified under the Damage Tolerance concept. This philosophy a priori admits the presence of hidden manufacturing defects or service-induced impact damage in the fairing. The structural-strength engineer is obliged to mathematically prove that these defects will not attain critical size over the prescribed number of rocket operating cycles.

The application of the XFEM algorithms and the modified Paris laws developed in Chapter 3 enables the creation of a digital twin of the defect. The integration of PSD into crack-growth models provides the possibility of calculating the exact residual life of a composite fairing in terms of the number of admissible launches. This directly forms the economic substantiation of the life-cycle cost of a reusable system.

The transition observed in the aerospace industry from a deterministic to a probabilistic approach is conditioned by the fact that deterministic calculations with rigidly prescribed growth constants and artificially overestimated initial crack sizes often show inadmissibility of operation for a part that, in practice, possesses an enormous survivability reserve.

The developed stochastic methodology described in Section 3.4 is ideally integrated into the RDTA framework. It enables treating the scatter in the physico-mechanical properties of PCM, the dispersion of initial defect sizes, and the random nature of acoustic pressure pulsations as probability distributions. By applying Monte Carlo simulation methods, engineers obtain the probability density of structural failure at each flight cycle.

This statistical analysis is critical for regulating interflight maintenance procedures. Knowing the maximum crack-growth rate under launch acoustics, engineers substantiate the required resolution of nondestructive evaluation methods, such as phased-array ultrasonic testing or laser vibrometry.

A profound understanding of the physics of fiber orientation's influence on crack arrest, described in Section 3.2, opens the door to targeted optimization of the payload fairing's mass characteristics. Instead of uniform thickening of the skin to reduce global stresses, designers may adopt a regionally adapted layup.

In zones of maximum concentration of flexural vibroacoustic stresses, for example, in the regions of circumferential frames or ply-drops, special damping layers or plies oriented at 90° are introduced, artificially blocking the growth of interlaminar delaminations through the bridging mechanism. This allows redistribution of energetic fluxes within the laminate, increasing the overall energy capacity of the structure without adding superfluous weight. Reduction of the dry mass of a composite fairing by even 10–15% owing to the abandonment of excessive safety margins directly translates into increased payload capacity, which is the principal driver of the competitiveness of commercial RLV operators.

Thus, the mathematical apparatus of fracture mechanics for orthotropic media presented in Chapter 3 serves as the basis for predictive analytics, certification, and economic optimization of next-generation reusable space transportation systems.

# CHAPTER 4.
# Methodology for Assessing the Survivability and Residual Life of Composite Aerospace Structures

The contemporary paradigm for developing reusable space transportation systems necessitates revising approaches to ensuring structural integrity. The transition from the safe-life concept, which presupposes the absence of defects throughout the entire service life, to the damage-tolerant concept is driven by both the physical properties of polymer composites and stringent economic imperatives. Under conditions of stochastic vibroacoustic loading, where the number of loading cycles during a single launch is counted in millions, traditional deterministic methods of strength assessment can result in either inadmissible risk or excessive structural mass.

The methodology presented in this chapter forms a unified analytical and technological cycle, enabling integration of data on external loading, the current condition of the material, and the stochastic nature of fracture to support substantiated engineering decisions on life extension or repair.

## 4.1. Integrated Life-Assessment Algorithm

The algorithm constitutes a sequential multilevel procedure ensuring the translation of macroscopic flight parameters into microstructural changes in the material. In contrast to existing approaches, this algorithm seamlessly unites the results of vibroacoustic modeling presented in Chapter 2 with the fracture mechanics of orthotropic media presented in Chapter 3.

The algorithm's logic is based on five successive stages, each of which is critical for obtaining a reliable prediction of residual life.

The first stage is the formation of the spectral load profile. At this stage, on the basis of flight telemetry or computational models, the power spectral density matrix, PSD, of the external acoustic pressure is formed. A critical aspect here is the consideration of the acoustic fill effect, which significantly alters the modal density of the internal fairing volume when a payload is present. The algorithm accounts for the spatial correlation CPSD, enabling identification of the frequency ranges in which the acoustic field's energy is transferred with maximal efficiency to the shell's flexural modes.

The second stage is the calculation of the global dynamic response. Using a hybrid FE-SEA, Finite Element - Statistical Energy Analysis, model, the stress-strain state of the entire fairing is calculated. The objective of this stage is to determine stress-concentration zones where the RMS stresses in the PCM plies attain threshold fatigue values. Particular attention is devoted to geometric irregularities: circumferential frames, ply-drop regions, and the vicinity of technological hatches.

The third stage is precision submodeling of defects. The identified critical zones are subjected to a procedure of structural zooming. A local volume is extracted from the global shell model and discretized using solid elements to provide a detailed description of interlaminar interactions. The mathematical connection between the models is ensured through displacement interpolation along the cut boundaries. At this stage, the parameters of real defects obtained during nondestructive inspection are introduced into the model. For accurate modeling, higher-order shape functions are used to minimize approximation errors in singularity zones.

The fourth stage is the probabilistic prediction of damage kinetics. This stage constitutes the core of the methodology. Since vibroacoustic loading is random in character, crack-growth increments are calculated in the frequency domain using Dirlik's method. The algorithm transforms the PSD of local stresses into the probability density function of cycle amplitudes. Thereafter, using the modified Paris law or the NASGRO equation for orthotropic media, the expected defect-growth rate is computed. The fiber crack-arrest effect and the mixed-mode character of fracture, Mixed-Mode I/II/III, are taken into account.

The fifth stage is synthesis and life decision-making. At the final stage, the cumulative probability of failure is formed. The algorithm compares the current calculated defect size with the critical size determined in Section 4.2. The residual life is expressed as the number of safe launches until the defect attains 80% of the critical value. The most important innovation here is the consideration of the Jensen gap, a mathematical confirmation that random variations in defectiveness reduce structural strength disproportionately more severely than their mean values. The logical structure of the integrated algorithm for assessing the life of the RLV composite fairing is shown in Figure 18.

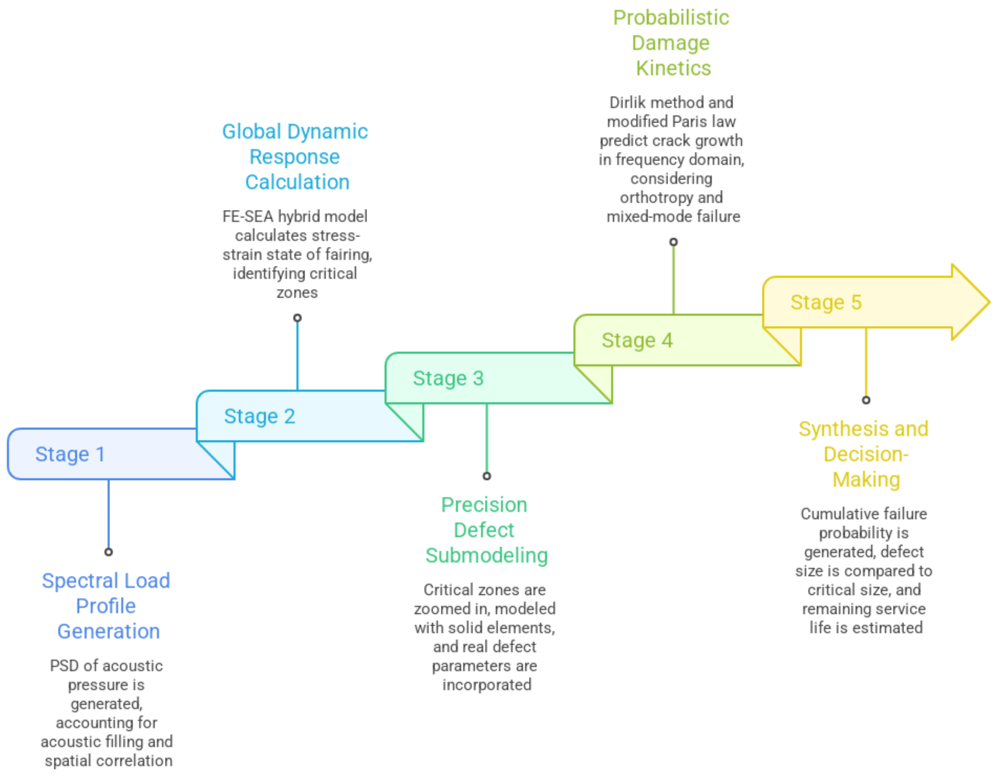


**Fig. 18.** Logical structure of the integrated algorithm for assessing the life of the RLV composite fairing

Table 9 presents the key characteristics of the input data for each stage of the algorithm, ensuring its reliability.

**Table 9. The relationship between parameters at different levels of the algorithm hierarchy**

| Analysis Level | Key Input Parameter | Physical Mechanism | Resulting Metric |
|---|---|---|---|
| Macro, System | Acoustic pressure PSD | Diffuse field, shell resonance | Stress spectral density |
| Meso, Structural | Submodel geometry | Stress concentration at nodes | Boundary conditions for the crack |
| Micro, Material | Fracture toughness energy | Interlaminar shear, delamination | Defect growth rate |
| Statistical | Probability of Detection, POD | Inspection uncertainty | Confidence interval of service life |

## 4.2. Assessment of Critical Defect Sizes

Determining the limiting admissible critical defect sizes is the most consequential stage of the methodology, since an error in this calculation may lead to catastrophic failure of the structure in flight. In composite RLV shells, the critical size is defined as the magnitude of damage at which the structure loses the ability to withstand the design ultimate loads or undergoes a sudden loss of stability.

For multilayer carbon-fiber fairing structures, several failure scenarios are critical, each associated with a loss of load-bearing capacity due to hidden or manifest defects.

The first scenario is associated with loss of stability of the detached skin. In the presence of interlaminar delamination and under the action of compressive membrane stresses arising, for example, in the Max-Q regime or under axial overload, the thin part of the laminate above the defect region loses stability. As a result, normal opening stresses increase at the delamination tip. This creates conditions for rapid, practically avalanche-like propagation of the defect.

The second critical scenario is characteristic of sandwich panels with honeycomb core and is associated with face-sheet wrinkling. In this case, the determining quantity is the size of the disbond. When the area of such a zone exceeds the admissible limit, the skin loses local stability. Further development of the process leads to the destruction of the honeycomb core and, consequently, to a degradation of the structure's load-bearing properties.

The third scenario is caused by the reduction in compression-after-impact strength, that is, CAI. Impact damage of the BVID type, which may be barely discernible upon external inspection, is often accompanied by a developed network of internal delaminations. In this case, the critical parameter becomes the diameter of the damaged zone. It is precisely this that determines the moment at which the residual strength of the structure decreases below the level corresponding to a 1.5-fold safety margin relative to operational loads.

Mathematically, the critical state is determined through the balance of released strain energy. The crack-stability condition has the form:

$$G_{total} = G_I + G_{II} + G_{III} \leq G_c$$

where $G_c$ is the critical fracture toughness determined by the Benzeggagh–Kenane criterion for mixed modes.

For cylindrical fairing shells, the critical defect size correlates strongly with the radius-to-thickness ratio. Numerical studies show that, with increasing delamination area, the critical buckling load decreases to a certain plateau, which determines the survivability of the structure (Venkat et al., 2025). Table 10 shows typical values of critical defect sizes for a medium-class RLV fairing.

**Table 10. Typical values of critical defect sizes for a medium-class RLV fairing (Tafreshi, 2004)**

| Defect Type | Location | Critical Area / Length | Strength Reduction | Main Risk Factor |
|---|---|---|---|---|
| Interlaminar delamination | Mid-surface | 50–75 mm, diameter | 0.60–0.70 | Skin buckling |
| Porosity zone, >3% | Fastener attachment points | 1200–1500 mm² | 0.80–0.85 | Interlaminar shear in the matrix |
| Impact damage | Conical section | Depth > 1.2 mm | 0.50–0.65 | Brittle failure at Max-Q |
| Honeycomb disbond | Sandwich panel | 100–120 mm, diameter | 0.75–0.80 | Wrinkling |

It is important to note that the methodology prescribes setting the operational defect-size limit to 0.75-0.8 times the calculated critical value. This margin is necessary to compensate for uncertainties in material properties and NDT errors.

A simple numerical example can illustrate the engineering meaning of this requirement. Let the calculated critical size of an interlaminar delamination in the structural zone under consideration be $a_{cr} = 20\ mm$. If the operational defect limit is defined using a factor of 0.8, then $a_{lim} = 0.8 \times 20 = 16\ mm$.

Assume that a nondestructive inspection performed before the next flight detects a defect of 13 mm. In that case, the remaining margin up to the operational limit is $16 - 13 = 3\ mm$. If the average predicted defect growth rate is approximately 1.08 mm per launch, the defect may reach the operational limit after $3/1.08 \approx 2.8$ launches. Thus, the structure may formally remain acceptable at the current inspection stage, yet the result clearly indicates that the available life margin is limited to approximately two to three additional flights under the assumed loading conditions.

## 4.3. Recommendations for Nondestructive Evaluation

In reusable programs, nondestructive evaluation ceases to be perceived as a final quality-assurance procedure and becomes a dynamic instrument for technical-condition monitoring. Within the framework of the proposed methodology, its principal task consists of providing quantitative data on defect geometry for the computational module intended to assess residual life.

The practical role of nondestructive inspection may be clarified by a simple numerical example. Assume that the inspection method employed in the maintenance procedure is capable of reliably detecting defects with a characteristic size of 6 mm or greater. If the critical defect size for the structural zone is 20 mm and the operational limit is 16 mm, then the effectively controllable safety window between the reliably detectable defect and the operational limit is $16 - 6 = 10\ mm$.

If the mean predicted defect growth rate is 1.08 mm per launch, this corresponds to approximately $10 / 1.08 \approx 9$ launches. However, if a more conservative defect growth estimate of 1.6 mm per launch is adopted, the same inspection window is reduced to $10 / 1.6 \approx 6$ launches. This example demonstrates that inspection intervals should be defined rather on the basis of an upper-bound or conservative growth scenario.

For composite fairings, it is advisable to use a combination of inspection methods to cover different defect types. Ultrasonic testing using phased arrays is regarded as the principal method of quantitative mapping of delaminations and assessment of porosity level. The use of phased arrays enables rapid scanning of large fairing surfaces with automatic C-scan generation. The method demonstrates sensitivity to depth defects of 0.5 mm. X-ray computed tomography is recommended for local inspection of the most critical zones, including separation joints, pyrotechnic bolt installation sites, and metallic frames. This method is especially important for detecting matrix cracks and fiber breaks, which may remain hidden in the ultrasonic signal. Automated Digital Tap Testing is used as an expedient method for initial detection of delamination zones and honeycomb-core disbonds. Contemporary digital hammers generate a quantitative signal as a force-versus-time function. This allows the subjective factor to be excluded from the interpretation of inspection results.

The key parameter determining the reliability of nondestructive evaluation is the Probability of Detection, POD. In accordance with NASA-STD-5009, confirmation of the 90/95 POD level is required for critical components (NASA, 2023). This means defect detection with a 90% probability at a 95% confidence level.

The methodology of ultrasonic signal processing includes several interrelated stages. First, feature extraction is performed in three domains. The analysis is conducted in the time domain, accounting for amplitude and time delay. Next, the frequency domain is considered using FFT and attenuation parameters. In addition, wavelet analysis based on Wavelet decomposition is applied. The next stage involves the use of machine-learning methods. For automatic defect segmentation on C-scans and classification of their type, it is proposed to use convolutional neural networks. Such an approach allows distinguishing, for example, delamination from protective-film inclusion.

Contemporary studies on the automated processing of phased-array data confirm the practical viability of this approach. For the task of delamination detection in composites, on a real ultrasonic data array, a mean average precision of 98.97% is reported, which notably surpasses classical manual signal interpretation and renders the integration of AI approaches into the digital life-assessment loop entirely well-founded (Cheng et al., 2024).

The final stage becomes the reconstruction of the three-dimensional geometry of the defect. Nondestructive-evaluation data are directly imported into the finite-element model, in particular into the submodel for residual-strength calculation. As a result, a digital twin of the defect is formed, which is used for subsequent analysis. The automated NDT data processing algorithm for state assessment is illustrated in Figure 19.

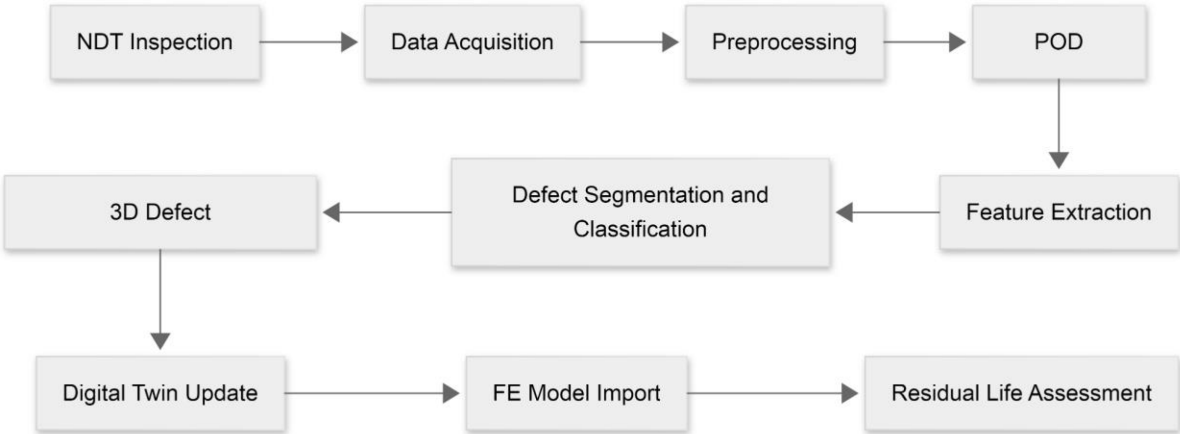


**Fig. 19.** Automated NDT data processing algorithm for state assessment

The integration of precision NDT and computational models enables abandoning fixed interflight regulations in favor of flexible work planning, where the scope of inspection is determined by flight telemetry results.

## 4.4. Practical Significance for RLV Programs

The economic efficiency of reusable systems directly depends on two factors: the cost of interflight servicing and the number of use cycles of expensive assemblies. The payload fairing is one of the largest and most expensive passive elements of the launch vehicle.

The application of the developed methodology makes it possible, on a substantiated basis, to increase the number of launches per article from the current 5-10 to 20-30 or more. This is achieved by precisely predicting defect kinetics, enabling the fairing to remain in service upon detection of minor delaminations.

The practical significance of this approach may be illustrated by a simple service-life scenario. Without a validated probabilistic residual-life assessment framework, a payload fairing may be conservatively withdrawn from service immediately after the detection of an 8 mm interlaminar defect, solely because its future growth behavior remains unknown. By contrast, if the proposed methodology predicts an average defect growth rate of approximately 1.08 mm per launch and an operational limit of 16 mm, the same defect may remain acceptable for several additional flights. In this case, the initially detected 8 mm defect would require approximately seven to eight launches to approach the operational limit. Even such a simplified example demonstrates how a validated life-assessment methodology can prevent premature rejection of expensive composite flight hardware.

According to SpaceX data, the cost of refurbishing a recovered fairing amounts to less than 10% of the cost of a new one (Brown, 2020). With 20-fold use, the specific fairing cost per launch decreases from USD 6 million to USD 300–400 thousand, which confers a colossal competitive advantage in the launch-services market.

The abandonment of conservative safety factors in favor of probabilistic calculations makes it possible to reduce fairing mass by 15-20%. For medium-class launch vehicles, this means the possibility of placing an additional 300-500 kg of payload into orbit. At a market launch price of 2500 - 3000 USD/kg, each launch yields additional revenue in the amount of approximately USD 1-1.5 million.

The use of validated computational models, digital twins, makes it possible to substantially reduce the volume of expensive full-scale testing in reverberant acoustic chambers. The transition to analytically demonstrated survivability accelerates the process of approving new fairing modifications for flight by regulators, which is critical under conditions of a rapidly changing commercial-launch market.

The created life-assessment methodology provides engineers with a predictive digital instrument. Precise modeling of defect kinetics enables verification that an existing microdelamination will not exceed limits under exposure to the acoustics of the next launch. This legitimizes abandoning the blind overestimation of laminate thicknesses for compensating for random AFP-layup manufacturing anomalies.

### 4.5. Universality and Scalability of the Methodology

The developed methodology was designed as an instrument applicable to a broad class of aerospace structures and international RLV programs. The scalability of the algorithms is confirmed by their effectiveness for products of differing dimensions. For small launch vehicles, such as Rocket Lab's Electron and Neutron, fully carbon-fiber structures are particularly important. They require precision consideration of AFP-layup specifics and of the influence of small curvature radii on defect growth. For heavy launch vehicles, including SpaceX Starship and SLS, fairings of up to 9–10 meters in diameter are considered. In this case, the methodology is scaled through the use of SEA methods for high-frequency acoustics and automated large-area NDT systems.

Although the principal attention is devoted to epoxy carbon-fiber composites, the energetic fracture criteria and spectral fatigue models preserve a universal character. The methodology may be recalibrated for thermoplastic composites, which demonstrate higher impact toughness and possess potential for rapid welding and repair at the launch site. It is also applicable to ceramic composites used in thermal protection panels for reusable stages. In this case, the methodology enables assessment of their thermoacoustic fatigue during reentry into dense atmospheric layers.

The methodology meets the stringent requirements of leading space agencies. Comparative analysis of international programs shows a growing demand for such instruments in China, within the LandSpace Zhuque-3 project, in India, in the RLV-TD program, and in Europe, in the Ariane Next project. The universality of NDT data-processing algorithms enables their integration into any existing quality management system. This ensures transparency and reproducibility of reliability-assessment results.

Thus, the methodology presented in Chapter 4 provides a reliable scientific and technological foundation for ensuring the safety and economic sustainability of future space transportation systems, linking fundamental materials science with the practical engineering of reusable spaceflight.

# CONCLUSION

The global aerospace industry is entering a phase of total commercialization and pragmatism, underpinned by the transition to reusable space transportation systems. However, the economic viability of this business model, which aims to reduce launch costs by orders of magnitude, is heavily dependent on the engineering community's ability to ensure the impeccable structural reliability of composite assemblies across dozens of high-intensity flight cycles. The present monograph is devoted to solving this critical scientific-applied problem: the development of a fundamentally substantiated probabilistic methodology for predicting the survivability and residual life of composite shell structures operating under extreme stochastic vibroacoustic loads.

Chapter 1 analyzed the ontological context of the PCM reliability problem in aerospace engineering. The complete inadequacy of traditional deterministic calculation methods for heterogeneous layered materials was demonstrated. The critical necessity of transition to the philosophy of damage tolerance, strictly regulated by advanced standards, was substantiated. It was shown that the stochastic nature of the occurrence of inevitable manufacturing defects, such as delaminations, porosity, and AFP-layup kinematic gaps, radically transforms the composite's strength distribution, according to Jensen’s inequality, forming unpredictable heavy tails in the probability of catastrophic failure.

Chapter 2 elucidated the complex physics of the formation of vibroacoustic loads. A validated hybrid computational modeling architecture was presented, uniting the classical finite element method for assessing low-frequency resonances with statistical energy analysis for reproducing the high-frequency diffuse acoustic field. This enabled high-precision localization of the zones of extreme dynamic stress concentration in orthotropic fairings, accounting for the nonlinear effects of acoustic cavity fill and transonic aerodynamic pressure.

Chapter 3 established a rigorous mathematical basis for the computational fracture mechanics of anisotropic media. The effectiveness of integrating isoparametric singular elements and XFEM together with VCCT for the precision calculation of the strain-energy release rate directly at the defect tip was substantiated. An approach was developed to adequately model mixed-mode fracture effects and the crack-arrest phenomenon induced by reinforcing fibers, a characteristic exclusively of PCM.

Chapter 4 synthesized the accumulated fundamental apparatus into an applied, stepwise algorithm for global-local submodeling and spectral life assessment. The inseparable mathematical and physical relationship was demonstrated among the spectrum of acoustic noise, the digital 3D reconstruction of defect geometry from automated nondestructive evaluation data, and the probabilistic laws of crack-growth kinetics, enabling computation of residual life in flight cycles.

The principal scientific contribution of the present work lies in the development of a comprehensive, cross-disciplinary methodology that consistently integrates deterministic continuum macromechanics with stochastic fracture microkinetics in orthotropic layered structures. The proposed approach establishes a closed and mathematically transparent analytical cycle, enabling direct translation of the power spectral density of external stochastic acoustic loading at the launch environment into probabilistic fatigue-growth behavior of hidden interlaminar delaminations. Furthermore, the developed methodology effectively resolves the fundamental problem of scale transition, bridging structural response at the level of tens of meters of the global fairing with damage processes occurring at sub-millimeter scales within the cohesive zone, while maintaining computational stability and ensuring robust algorithmic convergence.

From a practical and commercial standpoint, the created methodology constitutes a powerful systemic instrument for increasing economic profitability in the New Space industry. The integration of multimodal NDT data-fusion methods, such as the Fusion of ultrasonics and thermography, with virtual strength testing enables operators to avoid unjustified rejection of expensive fairings when stable microanomalies are detected. Economic analysis confirms that abandoning excessive conservative safety factors in favor of predictive survivability management saves operators millions of dollars in refurbishment procedures. Moreover, accurate calculation of critical defect sizes enables reducing the passive dry mass of the airframe by 5–10%, which directly translates into an increase in commercial payload. The implementation of this methodology also substantially reduces the timelines and budget for the certification of new launch vehicles, providing regulators with a reliable evidentiary basis.

The further evolution of the developed methodology is inseparably connected with the concept of total digitalization of the aerospace industry within Industry 4.0. The key vector of scientific development is the introduction of machine-learning and deep-learning algorithms for automated, real-time streaming processing of gigantic arrays of defectoscopic data. A strategically promising direction appears to be the physical integration of sensor networks, such as fiber Bragg gratings, FBG, and distributed piezoelectric acoustic-emission sensors, directly into the structure of the composite skin at the stage of automated layup. The transition from passive nondestructive evaluation to systems of active continuous condition monitoring will enable digital twins of fairings to self-update during flight, maximizing mission safety and bringing us closer to the era of fully autonomous, absolutely reliable, and economically perfected space transportation systems of the future.

# References

Abbasi, V., Ahmadi, M., Mohtarami, E., Karimi, J., & Saberi, F. (2024). Experimental and numerical failure mechanism evaluation of anisotropic rocks using extended finite element method. *Theoretical and Applied Fracture Mechanics*, *131*, 104411. https://doi.org/10.1016/j.tafmec.2024.104411

Adams, F. D., & Engle, R. M. (1985). A Damage Tolerance Approach for Structural Integrity of Aerospace Vehicles. In L. W. Masters (Ed.), *Problems in Service Life Prediction of Building and Construction Materials* (pp. 93–109). Springer Netherlands. https://doi.org/10.1007/9789400951259_6

Ahn, B., & Lee, S. (2022). Integrated Acoustic Analysis of Payload Fairing Using an FE-SEA Hybrid Method. *International Journal of Aeronautical and Space Sciences*, *24*(1), 1–8. https://doi.org/10.1007/s42405-022-00500-4

Alam, P., Mamalis, D., Robert, C., Floreani, C., & Ó Brádaigh, C. M. (2019). The fatigue of carbon fibre reinforced plastics - A review. *Composites Part B: Engineering*, *166*, 555–579. https://doi.org/10.1016/j.compositesb.2019.02.016

Alamry, A. (2024). Fatigue Damage and Analysis of Laminated Composites: A State-of-the-

art. *Journal of Engineering Research*, *13*(3), 2066–2076. https://doi.org/10.1016/j.jer.2024.09.006
Ansys. (n.d.). *Acoustic Analysis Guide* . Ansys. Retrieved March 3, 2026, from https://ansyshelp.ansys.com/public/account/secured?returnurl=//////Views/Secured/corp/v242/en/ans_acous/ans_acous.html
Ayatollahi, M. R., Nejati, M., & Ghouli, S. (2021). Crack tip fields in anisotropic planes: a review. *International Journal of Fracture*, *234*, 113–139. https://doi.org/10.1007/s10704-021-00559-2
Babaevskiy, P. G., Salienko, N. V., & Shatalin, A. A. (2024). Experimental Assessment of the Adequacy of Numerical Modeling of the Interlayer Crack Resistance of a Laminate Glass-Epoxy Composite under Combined Loading Mode I/II. *Inorganic Materials: Applied Research*, *15*(5), 1558–1564. https://doi.org/10.1134/s2075113324701260
Bi, S., Huang, Y., & Wang, H. (2024). General analytical solution for stress intensity factors of two asymmetrical radial cracks emanating from a single hole in an infinite isotropic plate. *Thin-Walled Structures*, *208*, 112759. https://doi.org/10.1016/j.tws.2024.112759
Bogenfeld, R., Freund, S., Dähne, S., Wunderlich, T., & Wille, T. (2024). Damage tolerance allowable calculation for the aircraft design with static ultimate load. *Composite Structures*, *329*, 117803. https://doi.org/10.1016/j.compstruct.2023.117803
Borgaonkar, A., Mandale, M., Potdar, S., & Chaitanya, Ch Sri. (2021). Statistical Energy Analysis Parameters Investigation of Composite Specimens Employing Theoretical and Experimental Approach. In S. Sahoo (Ed.), *Recent Advances in Layered Materials and Structures* (pp. 307–330). Springer Singapore. https://doi.org/10.1007/9789813345508_12
Brown, M. (2020, August 22). *SpaceX: Elon Musk breaks down the costs of reusable rockets*. Inverse. https://www.inverse.com/innovation/spacex-elon-musk-falcon-9-economics
Calabuig, G. J. D., Wilson, A., Bi, S., Vasile, M., Sippel, M., & Tajmar, M. (2024). Environmental life cycle assessment of reusable launch vehicle fleets: Large climate impact driven by rocket exhaust emissions. *Acta Astronautica*, *221*, 1–11. https://doi.org/10.1016/j.actaastro.2024.05.009
Cao, M., Zheng, X., Yan, L., & Ma, W. (2025). A Rationalized Enhancement of the Tsai-Wu Failure Criterion Considering the Stress States of Fibers and Matrix Simultaneously for the Bridging Model. *Acta Mechanica Solida Sinica*. https://doi.org/10.1007/s10338-025-00670-0
Chaudhari, T. S., Mathews, N. G., Mishra, A. K., Sahasrabuddhe, H. P., & Jaya, B. N. (2021). Energy Release Rate Formulations for Non-conventional Fracture Test Geometries. *JOM*, *73*(6), 1597–1606. https://doi.org/10.1007/s11837-021-04637-7
Cheng, X., Qi, H., Wu, Z., Zhao, L., Cech, M., & Hu, X. (2024). Automated Detection of Delamination Defects in Composite Laminates from Ultrasonic Images Based on Object Detection Networks. *Journal of Nondestructive Evaluation*, *43*(3), 94. https://doi.org/10.1007/s10921-024-01116-2
Chiarelli, M. R. (2025). Dynamic Response of Beams Under Random Loads. *Mathematics*, *13*(8), 1322. https://doi.org/10.3390/math13081322
Coherent Market Insights. (2025). *Reusable Launch Vehicle Market*. Coherent Market Insights. https://www.coherentmarketinsights.com/industry-reports/reusable-launch-vehicle-

market
Dash, B., Mahapatra, T. R., Mishra, P., Mishra, D., & R, M. S. (2025). A Review of Computational Methods for Vibroacoustic Analysis of Advanced Material Structures. *Archives of Computational Methods in Engineering*, *32*(4), 2187–2211. https://doi.org/10.1007/s11831024102045
Deng, J., Zhou, J., Wu, T., Liu, Z., & Wu, Z. (2023). Review and Assessment of Fatigue Delamination Damage of Laminated Composite Structures. *Materials*, *16*(24), 7677. https://doi.org/10.3390/ma16247677
Ding, S., Zhou, H., Liu, J., Zhang, X., & Li, G. (2023). Review of the development of the probabilistic damage tolerance assessment of life-limited parts in compliance with the airworthiness regulations. *Propulsion and Power Research*, *12*(3), 297–321. https://doi.org/10.1016/j.jppr.2023.08.001
Dinkler, D., Kowalsky, U., Dinkler, D., & Kowalsky, U. (2024). Isoparametric Elements. In *Introduction to Finite Element Methods* (pp. 215–228). Springer Fachmedien Wiesbaden. https://doi.org/10.1007/9783658427429_12
Dirlik, T., & Benasciutti, D. (2021). Dirlik and Tovo-Benasciutti Spectral Methods in Vibration Fatigue: A Review with a Historical Perspective. *Metals*, *11*(9), 1333. https://doi.org/10.3390/met11091333
Dróżdż, A., Niegodajew, P., Romańczyk, M., & Elsner, W. (2023). Convection velocity in turbulent boundary layers under adverse pressure gradient. *Experimental Thermal and Fluid Science*, *145*, 110900. https://doi.org/10.1016/j.expthermflusci.2023.110900
Du, T., Qin, T., Li, D., Wei, W., Zhang, J., Meng, Q., & Miao, X. (2025). Lifecycle Cost Estimation and Critical Parameters Analysis for Reusable Launch Vehicle. *Advances in Astronautics*, *8*(2), 89–106. https://doi.org/10.1007/s42423-025-00187-1
Elhajjar, R. (2025). Fat-tailed failure strength distributions and manufacturing defects in advanced composites. *Scientific Reports*, *15*, 25977. https://doi.org/10.1038/s41598-025-06693-4
Escartí-Guillem, M. S., Garcia-Raffi, L. M., & Hoyas, S. (2024). Review of launcher lift-off noise prediction and mitigation. *Results in Engineering*, *23*, 102679. https://doi.org/10.1016/j.rineng.2024.102679
Escartí-Guillem, M. S., Hoyas, S., & García-Raffi, L. M. (2023). Deflector shape impact on aero-acoustic noise generation and propagation. *Acta Astronautica*, *213*, 385–391. https://doi.org/10.1016/j.actaastro.2023.09.005
Fakoor, M., Ghodsi, S., Izadi, S. M. H., & Daneshjoo, Z. (2025). Exploring Fracture Toughness in the Damage Zone of Fiber-Reinforced Composites: A Study on Crack Orientation Effects. *Arabian Journal for Science and Engineering*. https://doi.org/10.1007/s13369-025-10272-0
Fu, Y., & Yao, X. (2022). A review on manufacturing defects and their detection of fiber reinforced resin matrix composites. *Composites Part C: Open Access*, *8*, 100276. https://doi.org/10.1016/j.jcomc.2022.100276
Gao, X., Sitharam, M., & Roitberg, A. E. (2020). *Bounds on the Jensen Gap, and Implications for Mean-Concentrated Distributions*. ArXiv. https://arxiv.org/abs/1712.05267
Gee, K. L., Hart, G. W., Cunningham, C. F., Anderson, M. C., Bassett, M. S., Mathews, L. T., Durrant, J. T., Moats, L. T., Coyle, W. L., Kellison, M. S., & Kuffskie, M. J. (2023).

Space Launch System acoustics: Far-field noise measurements of the Artemis-I launch. *JASA Express Letters*, *3*(2), 023601. https://doi.org/10.1121/10.0016878

GlobeNewswire. (2025, June 13). *Reusable Launch Vehicle Research Report 2025-2034*. GlobeNewswire. https://www.globenewswire.com/news-release/2025/06/13/3098898/28124/en/Reusable-Launch-Vehicle-Research-Report-2025-2034-Asia-and-Europe-Step-Up-in-Global-RLV-Market-with-Innovative-Prototypes.html

Gümüş, M. S., Erdemir, A., Alver, V., & Kalyoncu, M. (2021). Experimental evaluation of different spectral methods for damage estimation of an electrical panel bracket mounted on a military wheeled vehicle. *Journal of Mechanical Science and Technology*, *35*(12), 5561–5569. https://doi.org/10.1007/s12206-021-1127-6

Guo, F., Li, Y., Chen, Y., Liu, P., & Wang, X. (2025). Investigation of the Stress Intensity Factor in Heterogeneous Materials Based on the Postprocessing Routine of Commercial Finite Element Software. *Applied Sciences*, *15*(11), 5827. https://doi.org/10.3390/app15115827

Hoole, J., Sartor, P., Booker, J., Cooper, J., Gogouvitis, Xenofon V, Ghouali, A., & Kyle, S. R. (2020). A Framework to Implement Probabilistic Fatigue Design of SafeLife Components. In A. Niepokolczycki & J. Komorowski (Eds.), *ICAF 2019 – Structural Integrity in the Age of Additive Manufacturing* (pp. 321–335). Springer International Publishing.

Huang, T., & Bobyr, M. (2023). A Review of Delamination Damage of Composite Materials. *Journal of Composites Science*, *7*(11), 468. https://doi.org/10.3390/jcs7110468

Hughes, W., Mcnelis, A., & Mcnelis, M. (2014). *Acoustic Test Characterization of Melamine Foam for Usage in NASA's Payload Fairing Acoustic Attenuation Systems*. https://ntrs.nasa.gov/api/citations/20150006719/downloads/20150006719.pdf

Hwu, C., & Becker, W. (2022). Stroh formalism for various types of materials and deformations. *Journal of Mechanics*, *38*, 433–444. https://doi.org/10.1093/jom/ufac031

JAXA. (2022). *Technical Standard for High-Pressure Gas Equipment for Space Use* (JERG-0-001F(E)). JAXA. https://sma.jaxa.jp/TechDoc/Docs/E_JAXA-JERG-0-001F.pdf

Kaddaha, M. A., Younes, R., & Lafon, P. (2021). Homogenization Method to Calculate the Stiffness Matrix of Laminated Composites. *Eng*, *2*(4), 416–434. https://doi.org/10.3390/eng2040026

Kalariya, Y., Beemaraj, S. B., & Salvi, A. (2023). Design and Optimization of Manufacturing Process of Polymer Composites Through Multiscale Cure Analysis and NSGA-II. *Integrating Materials and Manufacturing Innovation*, *12*(4), 321–337. https://doi.org/10.1007/s40192-023-00316-4

Kang, S.-Y., Jo, M.-S., Choi, J.-Y., & Yang, S. S. (2025). Cost Effectiveness of Reusable Launch Vehicles Depending on the Payload Capacity. *Aerospace*, *12*(5), 364–364. https://doi.org/10.3390/aerospace12050364

Kim, S.-J., Lee, S., & Hwang, I. (2022). A Methodology to Determine Composite Material Allowables and Design Values Using Building Block Approach. *Journal of the Korean Society for Aeronautical & Space Sciences*, *50*(6), 377–384. https://doi.org/10.5139/jksas.2022.50.6.377

Kukwi, T., Shan, C., Pengfei, L., Zhang, B., Leiyang, G., & Wang, Z. (2025). Continuous

Improvement in Composite Manufacturing: A Review of Automated Fiber Placement Process Evolution and Future Research Prospects. *Applied Composite Materials*, *32*, 1267–1314. https://doi.org/10.1007/s10443-025-10325-5

Kulkarni, N. M., & Lal, A. (2024). Effect of random variation in input parameter on cracked orthotropic plate using extended isogeometric analysis (XIGA) under thermomechanical loading. *Curved and Layered Structures*, *11*(1). https://doi.org/10.1515/cls-2024-0012

Li, Z., Gao, Z., & Liu, Y. (2024). Enriched Constant Elements in the Boundary Element Method for Solving 2D Acoustic Problems at Higher Frequencies. *Computer Modeling in Engineering & Sciences*, *138*(3), 2159–2175. https://doi.org/10.32604/cmes.2023.030920

Liu, L., Ripamonti, F., Corradi, R., & Rao, Z. (2022). On the experimental vibroacoustic modal analysis of a plate-cavity system. *Mechanical Systems and Signal Processing*, *180*, 109459. https://doi.org/10.1016/j.ymssp.2022.109459

Liu, R., Yu, Z., & Nasonov, F. (2023). Evaluations on VCCT and CZM methods of delamination propagation simulation for composite specimens. *Aerospace Systems*, *6*(4), 621–632. https://doi.org/10.1007/s42401-023-00231-8

Lv, F., Zhou, C.-Y., Cheng, R.-J., Miao, X.-T., & He, X.-H. (2018). A numerical analysis based on M-integral about the interaction of parallel surface cracks in an infinite plate. *Theoretical and Applied Fracture Mechanics*, *96*, 370–379. https://doi.org/10.1016/j.tafmec.2018.05.012

Maierhofer, J., Pippan, R., & Gänser, H.-P. . (2014). Modified NASGRO equation for physically short cracks. *International Journal of Fatigue*, *59*, 200–207. https://doi.org/10.1016/j.ijfatigue.2013.08.019

Mamat, R., Rashid, M. I. M., Syahir, A. Z., Yusop, A. F., & Tamimi, A. (2025). Carbon fibre for applications in aerospace: A review. *Journal of Alloys and Metallurgical Systems*, *12*, 100227. https://doi.org/10.1016/j.jalmes.2025.100227

Mishra, N. K., Harshitha, G., Reddy, G. Vamshi., Anirudh, P., Aashritha, V., & Govind, K. (2023). Computational study on rocket payload fairing. *Materials Today: Proceedings*, In Press. https://doi.org/10.1016/j.matpr.2023.06.244

Murčinková, Z., Postawa, P., & Winczek, J. (2022). Parameters Influence on the Dynamic Properties of Polymer-Matrix Composites Reinforced by Fibres, Particles, and Hybrids. *Polymers (Basel)*, *14*(15), 3060. https://doi.org/10.3390/polym14153060

Nair, S., Dasari, A., Yue, C., & Narasimalu, S. (2017). Failure Behavior of Unidirectional Composites under Compression Loading: Effect of Fiber Waviness. *Materials*, *10*(8), 909. https://doi.org/10.3390/ma10080909

NASA. (2023). *Nondestructive evaluation requirements for fracture-critical metallic components* (NASA-STD-5009C). NASA. https://standards.nasa.gov/sites/default/files/standards/NASA/C/0/2023-08-03-NASA-STD-5009C-Approved.pdf

NASA. (2025). *Fracture Control Requirements for Spaceflight Hardware* (NASA-STD-5019A w/CHANGE 4). https://standards.nasa.gov/sites/default/files/standards/NASA/w/CHANGE-4/4/NASA-STD-5019A-w-Change-4-Revalidated-2025-09-05.pdf

Parker, P., Koshti, A., Forsyth, D., Suits, M., Walker, J., & Prosser, W. (2023). NASA NDE Fracture Critical Detectable Flaw Sizes History and Methodology. *Proceedings of 31st ICAF Symposium*. https://www.icaf.aero/icaf2023/proceedings/documents/12.pdf

Pazhani, A., Salman, S. S., Venkatraman, M., Patel, A., Xavior, M. A., Batako, A., Paulsamy, J., & Jayaseelan, J. (2024). Dynamic FEA Analysis of the Super Lightweight External Cryogenic Fuel Tank (SLWT) Made of Aluminium Alloy 2195–Graphene Nano Composite for Launch Vehicle Aerospace Application. *Journal of Composites Science*, *8*(7), 260. https://doi.org/10.3390/jcs8070260

Peishi, Y., Junhua, Z., & Wanlin, G. (2021). Threedimensional Damage Tolerance Design: Outofplane Constraint Theory and Fatigue/Fracture Criteria. *Journal of Mechanical Engineering*, *57*(16), 87–105. https://doi.org/10.3901/JME.2021.16.087

Pelekis, S., Koutroubas, T., Blika, A., Berdelis, A., Karakolis, E., Ntanos, C., Spiliotis, E., & Askounis, D. (2025). Adversarial machine learning: a review of methods, tools, and critical industry sectors. *Artificial Intelligence Review*, *58*(8), 226. https://doi.org/10.1007/s10462025111474

Raju, I. S., Elliott, K. B., Hampton, R. W., Knight, N. F., Aggarwal, P., Engelstad, S. P., & Chang, J. B. (2010). Comparison of Requirements for Composite Structures for Aircraft and Space Applications . *Proceedings of Bangalore Composites Conference*, 1–15. https://ntrs.nasa.gov/api/citations/20110005521/downloads/20110005521.pdf

Russell, D. A. (n.d.). *Dispersion of Flexural Waves*. PSU. Retrieved March 7, 2026, from https://www.acs.psu.edu/drussell/Demos/Dispersion/Flexural.html

Saouma, V. E., & Amin, H. M. (2021). Finite Element Modeling of Cracks. In *Aging, Shaking, and Cracking of Infrastructures: From Mechanics to Concrete Dams and Nuclear Structures* (pp. 317–350). Springer International Publishing. https://doi.org/10.1007/9783030574345_14

Sayyad, A. S., Ghugal, Y. M., & Kant, T. (2022). Flexural mode, thickness-shear mode and thickness-twist mode frequencies of laminated composite shells of double curvature. *Composite Structures*, *291*, 115577. https://doi.org/10.1016/j.compstruct.2022.115577

Shearer, L., & Bittinger, S. (2022, June 28). *Payload Fairing Acoustic Trade Study: Fill Effect Modeling*. NASA. https://ntrs.nasa.gov/citations/20220008036

Shi, F.-T., Shang, D.-G., Wu, S.-D., Hao, G.-C., Zhou, C., Ma, J.-X., & Ma, Z.-P. (2025). Fatigue life prediction method based on Rayleigh model modified with spectral width coefficient for arbitrary bandwidth signals. *Measurement*, *251*, 117317. https://doi.org/10.1016/j.measurement.2025.117317

Shimazaki, S., & Shi, Q. (2021). A new method to specify the mitigated acoustic test conditions from flight telemetry based on the equivalence of vibro-acoustic response. *CEAS Space Journal*, *15*, 329–342. https://doi.org/10.1007/s12567-021-00410-3

Shonkwiler, S., Li, X., Fenrich, R., & McMains, S. (2023). Deep reinforcement learning for stacking sequence optimization of composite laminates. *Manufacturing Letters*, *35*, 1203–1213. https://doi.org/10.1016/j.mfglet.2023.08.133

Space Foundation. (2025, July 22). *The Space Report 2025*. Space Foundation. https://www.spacefoundation.org/2025/07/22/the-space-report-2025-q2/

Tafreshi, A. (2004). Delamination buckling and postbuckling in composite cylindrical shells under external pressure. *Thin-Walled Structures*, *42*(10), 1379–1404.

https://doi.org/10.1016/j.tws.2004.05.008
Taheri, F., Ghiaskar, A., & Chowdhury, S. A. (2025). Flexural and Shear Behavior of Basalt-Recyclamine Composites: A Comparative Study with Conventional Epoxy Systems. *Applied Composite Materials*, *32*(6), 2687–2716. https://doi.org/10.1007/s10443-025-10370-0
Taheri, H., & Hassen, A. (2019). Nondestructive Ultrasonic Inspection of Composite Materials: a Comparative Advantage of Phased Array Ultrasonic. *Applied Sciences*, *9*(8), 1628. https://doi.org/10.3390/app9081628
Tai, J. L., Thariq, M., Shahar, F. S., Yidris, N., & Basri, A. A. (2024). Exploring Probability of Detection (POD) Analysis in Nondestructive Testing: A Comprehensive Review and Potential Applications in Phased Array Ultrasonic Corrosion Mapping. *Pertanika Journal of Science & Technology*, *32*(5), 2165–2191. https://doi.org/10.47836/pjst.32.5.14
Tavaf, V., & Banerjee, S. (2022). Effect of Defects Part I: Degradation of Constitutive Coefficients as an Input to the Composite Failure Model with Microvoids and Porosity. *Journal of Composites Science*, *6*(2), 37. https://doi.org/10.3390/jcs6020037
Towner, R., & Band, J. (2012). An Analysis Technique/Automated Tool for Comparing and Tracking Analysis Modes of Different Finite Element Models. *53rd AIAA/ASME/ASCE/AHS/ASC Structures, Structural Dynamics and Materials Conference*. https://doi.org/10.2514/6.2012-1987
Upganlawar, S., & Anasane, Sandeep S. (2026). Enhanced Payload Fairing Design: Integrating CFRP and GFRP for Optimal Performance. In G. Raghavendra, K. B. Aswani, & M. Gupta (Eds.), *Recent Trends in Manufacturing Engineering* (pp. 297–307). Springer Nature Singapore.
Van hoorickx, C., & Reynders, E. P. B. (2022). Numerical realization of diffuse sound pressure fields using prolate spheroidal wave functions. *The Journal of the Acoustical Society of America*, *151*(3), 1710–1721. https://doi.org/10.1121/10.0009764
Vellwock, A. E., & Libonati, F. (2024). XFEM for Composites, Biological, and Bioinspired Materials: A Review. *Materials*, *17*(3), 745. https://doi.org/10.3390/ma17030745
Venkat, S. S., Scheffler, S., Anilkumar, P. M., Baranger, E., & Rolfes, R. (2025). Effect of delamination defects on buckling and growth characteristics in composite laminates. *Composite Structures*, *369*, 119245. https://doi.org/10.1016/j.compstruct.2025.119245
Wagenblast, B. N., & Bettinger, R. A. (2024). Statistical reliability estimation of space launch vehicles: 2000–2022. *Journal of Space Safety Engineering*, *11*(4), 573–589. https://doi.org/10.1016/j.jsse.2024.10.001
Wang, K., Wang, J., Liu, Z., Zhang, S., Zhang, B., & Quan, W. (2024). Thermal modal analysis of hypersonic composite wing on transient aerodynamic heating. *Scientific Reports*, *14*, 11012. https://doi.org/10.1038/s41598-024-61900-y
Yang, W., Feng, X.-Q., & Gao, H. (2026). Outstanding issues and emerging frontiers in fracture mechanics. *International Journal of Fracture*, *250*, 10. https://doi.org/10.1007/s10704-025-00907-6
Zotter, F., Riedel, S., Gölles, L., & Frank, M. (2024). Diffuse sound field synthesis: Ideal source layers. *Acta Acustica*, *8*, 34. https://doi.org/10.1051/aacus/2024023